

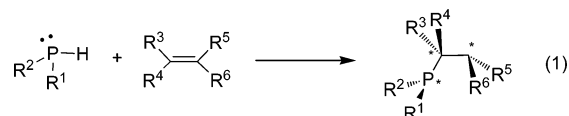
Enantioselective Addition of Secondary Phosphines to
Methacrylonitrile: Catalysis and MechanismAaron D. Sadow[†] and Antonio Togni*Contribution from the Department of Chemistry and Applied Biosciences,
Swiss Federal Institute of Technology, ETH Hönggerberg, CH-8093 Zürich, Switzerland

Received August 12, 2005; E-mail: togni@inorg.chem.ethz.ch

Abstract: A highly enantioselective intermolecular hydrophosphination reaction is described. The (Pigiphos)-nickel(II)-catalyzed reaction of secondary phosphines and methacrylonitrile gives chiral 2-cyanopropylphosphines in good yield and high enantiomeric excess (ee's up to 94%; (*R*)-(*S*)-Pigiphos = bis{(*R*)-1-[(*S*)-2-(diphenylphosphino)ferrocenyl]ethyl}cyclohexylphosphine). We propose a mechanism involving coordination of methacrylonitrile to the dicationic nickel catalyst followed by 1,4-addition of the phosphine, and then, rate-determining proton transfer. This mechanism is supported by (a) the experimentally determined rate law (rate = $k[\text{Ni}][\text{methacrylonitrile}][t\text{-Bu}_2\text{PH}]$), (b) a large primary deuterium isotope effect $k_{\text{H}}/k_{\text{D}} = 4.6(1)$ for the addition of $t\text{-Bu}_2\text{PH(D)}$ at 28.3 °C in toluene- d_6 , (c) the isolation and characterization of the species $[\text{Ni}(\kappa^3\text{-Pigiphos})(\kappa\text{-N-methacrylonitrile})]^{2+}$, and (d) DFT calculations of model compounds.

Introduction

Chiral phosphines are valuable as ligands in numerous important catalytic asymmetric processes.¹ Intense research efforts have produced many classes of chiral phosphines with diverse steric and electronic properties, and researchers have examined how these properties influence activity and stereoselectivity in catalysis. Given the recent rapid development of new methods in asymmetric catalysis and the prominence of chiral phosphines in this area of chemistry, it is surprising that few catalytic asymmetric syntheses of chiral phosphines have been described.² Instead, enantiopure phosphines are most commonly prepared either via stereospecific reactions of resolved starting materials or through routes which require an additional resolution step, such as a fractional crystallization of diastereomers.³ Stereoselective transition-metal catalysis could provide methods for the preparation of functionally and structurally diverse chiral phosphine ligands. Recent successes in this area include a dynamic kinetic resolution of racemic secondary phosphines in a Pd-catalyzed P–H/aryl halide coupling for the preparation of P-stereogenic phosphines.³ Catalytic asymmetric hydrophosphination of olefins is potentially an alternative and efficient synthetic route to chiral phosphines (eq 1).⁴



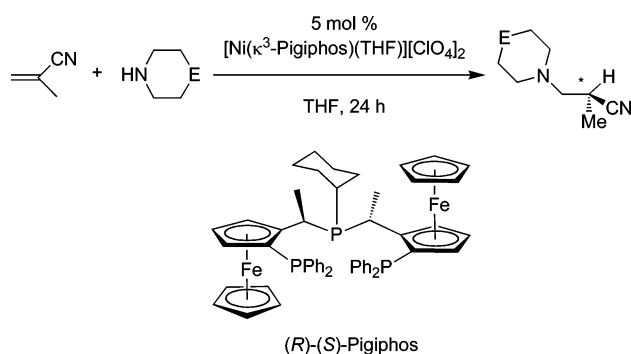
Base- and radical-promoted hydrophosphination of acrylonitrile with PH_3 was first reported in 1959 for the synthesis of $\text{H}_n\text{P}(\text{CH}_2\text{CH}_2\text{CN})_{3-n}$ mixtures,⁵ and later work has shown that these types of reactions are useful in stereospecific preparations of optically pure chiral phosphines. For example, stereospecific hydrophosphination of enantiopure norbornene derivatives is catalyzed by KOt-Bu .⁶ Transition-metal catalyses often show high selectivities, and accordingly, Pt complexes catalyze the hydrophosphination of acrylonitrile to form primarily $\text{P}(\text{CH}_2\text{CH}_2\text{CN})_3$.⁷ The mechanism of this reaction was proposed to involve oxidative addition of P–H bonds onto Pt(0) complexes followed by olefin insertion into the Pt-PR_2 bond.^{7,8} With the use of this strategy, stereoselective methacrylonitrile insertion involving $[\text{Pt}(\text{Duphos})(\text{PR}_2)\text{H}]$ was incorporated into a catalytic enantioselective hydrophosphination to give chiral 2-cyanopropyl phosphines with ee's up to 27%.⁹ This “phosphine-activation” mechanism is ubiquitous in metal-catalyzed asymmetric alkene hydrophosphination. A second prominent system

[†] Present address: Department of Chemistry, 1605 Gilman Hall, Iowa State University, Ames, IA 50011-3111.

- (1) *Catalytic Asymmetric Synthesis*; Ojima, I. Ed.; VCH: New York, 1993.
- (2) (a) Corbridge, P. E. C. *Studies in Inorganic Chemistry 20; Phosphorus: An Outline of its Chemistry, Biochemistry and Technology*, 5th ed.; Elsevier: Amsterdam, 1995. (b) Baillie, C.; Xiao, J. *Curr. Org. Chem.* **2003**, *7*, 477–514.
- (3) (a) Moncarz, J. R.; Laritcheva, N. F.; Glueck, D. S. *J. Am. Chem. Soc.* **2002**, *124*, 13356–13357. (b) Korff, C.; Helmchen, G. *Chem. Commun.* **2004**, 530–531. (c) Pican, S.; Gaumont, A.-C. *Chem. Commun.* **2005**, 2393–2395.
- (4) (a) Wicht, D. K.; Glueck, D. S. In *Catalytic Heterofunctionalization: From Hydroamination to Hydrozirconation*; Togni, A., Grützmacher, H., Eds.; Wiley-VCH: Weinheim, 2001; pp 143–169. (b) Tanaka, M. *Top. Curr. Chem.* **2004**, *232*, 25–54.

- (5) (a) Rauhut, M. M.; Hechenbleikner, I.; Currier, H. A.; Schaefer, R. C.; Wystrach, V. P. *J. Am. Chem. Soc.* **1959**, *81*, 1103–1107. (b) Rauhut, M. M.; Currier, H. A.; Semsel, A. M.; Wystrach, V. P. *J. Org. Chem.* **1961**, *26*, 5138–5135. (c) Habib, M.; Trujillo, H.; Alexander, C. A.; Storhoff, B. N. *Inorg. Chem.* **1985**, *24*, 2344–2349.
- (6) (a) Bunlaksanansorn, T.; Knochel, P. *Tetrahedron Lett.* **2002**, *43*, 5817–5819. (b) Bunlaksanansorn, T.; Knochel, P. *J. Org. Chem.* **2004**, *69*, 4595–4601.
- (7) (a) Costa, E.; Pringle, P. G.; Smith, M. B.; Worboys, K. *J. Chem. Soc., Dalton Trans.* **1997**, 4277–4282. (b) Pringle, P.; Smith, M. B. *Chem. Commun.* **1990**, 1701–1702.
- (8) (a) Wicht, D. K.; Kourkine, I. V.; Lew, B. M.; Nthenge, J. M.; Glueck, D. S. *J. Am. Chem. Soc.* **1997**, *119*, 5039–5040. (b) Wicht, D. K.; Kourkine, I. V.; Kovacic, I.; Glueck, D. S. *Organometallics* **1999**, *18*, 5381–5394.
- (9) Kovacic, I.; Wicht, D. K.; Grewal, N. S.; Glueck, D. S.; Incarvito, C. D.; Guzei, I. A.; Rheingold, A. L. *Organometallics* **2000**, *19*, 950–953.

Scheme 1



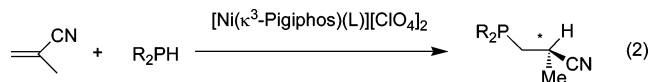
for asymmetric hydrophosphination is the organolanthanide-catalyzed cyclization of phosphino alkenes.¹⁰ In the context of the phosphine-activation mechanism, it is interesting that this intramolecular hydrophosphination and the corresponding hydroamination/cyclization proceed via similar mechanisms, in which a pendant olefin and the phosphido/amido lanthanide species react via diastereoselective migratory insertion.¹¹ Additionally, several noncatalytic asymmetric transition-metal-promoted hydrophosphinations have been described,¹² as well as several other nonasymmetric transition-metal catalyses.¹³

Our entry into catalytic asymmetric hydrophosphination developed from a longstanding interest in both chiral phosphine synthesis and catalytic asymmetric hydroamination reactions.^{14,15} Specifically, we reported that the nickel(II)-catalyzed intermolecular reaction of amines and methacrylonitrile affords the 2-cyanopropylamine products in high enantiomeric excesses (up to 96%),¹⁶ when using the tridentate phosphine ligand (R)-(S)-Pigiphos ((R)-(S)-Pigiphos = bis[(R)-1-[(S)-2-(diphenylphosphino)ferrocenyl]ethyl]cyclohexylphosphine, see Scheme 1).¹⁷

During investigations of this hydroamination reaction, several observations suggested that a Ni–olefin complex is involved in the catalytic cycle and that direct interaction of the amine substrate and the Ni center gives a catalytically inactive species. Therefore, we postulated that a Ni(II)-methacrylonitrile species reacts with the amine nucleophile to give the hydroamination

product. Because this mechanism could also apply to other nucleophiles, we began to examine reactions of phosphines and cyanoolefins in the presence of the dicationic [Ni(κ³-Pigiphos)-(THF)]²⁺ complex ([1]²⁺).

Herein, we describe the successful development of a Ni(II)-catalyzed hydrophosphination of methacrylonitrile to give 2-cyanopropyl phosphines (eq 2). The catalyst [Ni(κ³-Pigiphos)-



(L)]²⁺ affords the product with high conversion, yield, and enantiomeric excess, thus giving the most efficient intermolecular asymmetric catalytic hydrophosphination reported to date.¹⁸

Furthermore, preparative experiments are complemented by mechanistic investigations, including the synthesis and characterization of possible catalytic intermediates, kinetic studies, and modeling of the proposed intermediates by density functional theory (DFT) calculations. Our results implicate a mechanism in which a Ni-coordinated methacrylonitrile ligand is reactive toward nucleophilic attack. This “olefin-activation” mechanism has not previously been reported for catalytic hydrophosphination reactions and therefore offers alternative possibilities in comparison to the organolanthanide- and Pt-catalyzed phosphine-activation pathways.

Experimental Section

General. All manipulations were performed under an inert atmosphere using either standard Schlenk techniques or a N₂-filled glovebox. All solvents were distilled prior to use. The phosphines Ph₂PH, Cy₂PH, *t*-Bu₂PH, and *i*-Pr₂PH were synthesized by LiAlH₄ reduction of the corresponding chlorophosphines. (1-Ad)₂PH (1-Ad = 1-adamantyl) was synthesized by LiAlH₄ reduction of (1-Ad)₂P(O)Cl.¹⁹ (R)-(S)-Pigiphos (only the (R)-(S)-enantiomer was used throughout),¹⁷ [Ni(κ³-Pigiphos)-(THF)](ClO₄)₂ ([1](ClO₄)₂),¹⁶ (C₆H₅)₂PCH₂CH(CH₃)CN,⁹ [Pd₂(μ-Cl)₂-(κ²-(R)-(C₆H₄)CHMe(NMe₂))₂],²⁰ and [Pd₂(μ-Cl)₂-(κ²-(R)-(C₁₀H₆)-CHMe(NMe₂))₂]²¹ were synthesized according to published procedures. [Ni(H₂O)₆](ClO₄)₂, [Ni(H₂O)₆](BF₄)₂, NiCl₂, and NiBr₂ were purchased from Aldrich and used as received. Methacrylonitrile was distilled from CaCl₂, degassed with three freeze–pump–thaw cycles, and stored over activated 4 Å molecular sieves. Synthetic procedures and characterization data for the compounds Cy₂PCH₂CHMeCN (**2a**), *i*-Pr₂PCH₂CHMeCN (**2c**), *t*-Bu₂PCH₂CHMeCN (**2d**), (1-Ad)₂PCH₂CHMeCN (**2e**), and their naphthylamino Pd(II) complexes have previously been communicated.¹⁸ *Caution: Perchlorate salts are potentially explosive and appropriate safety measures should be taken.*

(EtMe₂C)₂PH. Mg turnings (9.90 g, 0.407 mol) were placed in a three-neck flask to which a reflux condenser and addition funnel were attached, and 150 mL of diethyl ether was added. A few flakes of iodine were added, and the mixture was stirred until the red color faded to yellow. 2-Bromo-2-methylbutane was placed in the addition funnel, degassed by sparging with argon, and added in a dropwise fashion to maintain slow reflux. The reaction mixture was heated to reflux for 1 h and then cooled to 0 °C. A solution of PCl₃ (8.89 mL) in OEt₂ was

- (10) (a) Douglass, M. R.; Marks, T. J. *J. Am. Chem. Soc.* **2000**, *122*, 1824–1825. (b) Douglass, M. R.; Stern, C. L.; Marks, T. J. *J. Am. Chem. Soc.* **122**, 123, 10211–10238. (c) Douglass, M. R.; Ogasawara, M.; Hong, S.; Metz, M. V.; Marks, T. J. *Organometallics* **2002**, *21*, 283–292. (d) Kawaoka, A. M.; Douglass, M. R.; Marks, T. J. *Organometallics* **2003**, *22*, 4630–4632. (e) Kawaoka, A. M.; Marks, T. J. *J. Am. Chem. Soc.* **2004**, *126*, 12764–12765. (f) Kawaoka, A. M.; Marks, T. J. *J. Am. Chem. Soc.* **2005**, *127*, 6311–6324.
- (11) Hong, S.; Marks, T. J. *Acc. Chem. Res.* **2004**, *37*, 673–686.
- (12) (a) Malisch, W.; Klüpfel, B.; Schumacher, D.; Nieger, M. *J. Organomet. Chem.* **2002**, *661*, 95–110. (b) Yeo, W.-C.; Tee, S.-T.; Tan, H.-B.; Tan, G.-K.; Koh, L. L.; Leung, P.-H. *Inorg. Chem.* **2004**, *43*, 8102–8109.
- (13) (a) Shulyupin, M. O.; Kazankova, M. A.; Beletskaya, I. P. *Org. Lett.* **2002**, *4*, 761–763. (b) Kazankova, M. A.; Shulyupin, M. O.; Beletskaya, I. P. *Synlett* **2003**, 2155–2158.
- (14) (a) Togni, A.; Breutel, C.; Schnyder, A.; Spindler, F.; Landert, H.; Tijani, A. *J. Am. Chem. Soc.* **1994**, *116*, 4062–4066. (b) Togni, A.; Burckhardt, U.; Gramlich, V.; Pregosin, P. S.; Salzmann, R. *J. Am. Chem. Soc.* **1996**, *118*, 1031–1037. (c) Togni, A. *Angew. Chem., Int. Ed. Engl.* **1996**, *35*, 1475–1477. (d) Togni, A.; Bieler, N.; Burckhardt, U.; Köllner, C.; Pioda, G.; Schneider, R.; Schnyder, A. *Pure Appl. Chem.* **1999**, *71*, 1531–1537.
- (15) (a) Dorta, R.; Egli, P.; Zürcher, F.; Togni, A. *J. Am. Chem. Soc.* **1997**, *119*, 122, 4089–4107. (b) Senn, H. M.; Blöchl, P. E.; Togni, A. *J. Am. Chem. Soc.* **2000**, *122*, 4098–4107.
- (16) (a) Fadini, L.; Togni, A. *Chem. Commun.* **2003**, 30–31. (b) Fadini, L., Ph.D. Thesis, No. 15593, ETH Zurich, 2004.
- (17) (a) Barbaro, P.; Togni, A. *Organometallics* **1995**, *14*, 3570–3573. (b) Barbaro, P.; Bianchini, C.; Togni, A. *Organometallics* **1997**, *16*, 3004–3014. (c) Barbaro, P.; Bianchini, C.; Oberhauser, W.; Togni, A. *J. Mol. Catal.* **1999**, *145*, 139–146. (d) Hintermann, L.; Perseghini, M.; Barbaro, P.; Togni, A. *Eur. J. Inorg. Chem.* **2003**, 601–609.

- (18) Sadow, A.; Haller, I.; Fadini, L.; Togni, A. *J. Am. Chem. Soc.* **2004**, *126*, 14704–14705.
- (19) (a) No., I. B.; Zotov, Y. L.; Karev, V. N. *Zh. Obshch. Khim.* **1990**, *60*, 1975–1999. (b) Goerlich, J. R.; Schmutzler, R. *Phosphorus, Sulfur Silicon Relat. Elem.* **1993**, *81*, 141–148.
- (20) (a) Otsuka, S.; Nakamura, A.; Kano, T.; Tani, K. *J. Am. Chem. Soc.* **1971**, *93*, 4301–4303. (b) Roberts, N. K.; Wild, S. B. *J. Am. Chem. Soc.* **1979**, *101*, 6254–6260. (c) Wild, S. B. *Coord. Chem. Rev.* **1997**, *166*, 291–311.
- (21) Tani, K.; Brown, L. D.; Ahmed, J.; Ibers, J. A.; Yokota, M.; Nakamura, A.; Otsuka, S. *J. Am. Chem. Soc.* **1977**, *99*, 7876–7886.

added slowly, and the mixture was allowed to warm to room temperature (r.t.) and then was heated to reflux for 2 h. The reaction mixture was filtered and purified by distillation (40 °C at 2×10^{-2} mbar). In a separate flask, OEt_2 (70 mL) was added to LiAlH_4 (3.59 g), and the flask was cooled to 0 °C. The distilled $(\text{EtMe}_2\text{C})_2\text{PCl}$ was added in a dropwise fashion to this mixture, and the reaction mixture was then heated to reflux overnight. Degassed water was added slowly (0 °C), and the mixture was filtered, dried over MgSO_4 , and distilled under reduced pressure. Yield: 5 g, 28%, density = 0.76 g/mL. ^1H NMR (C_6D_6 , 400 MHz): δ 3.12 (d, 1 H, HP, $^1J_{\text{PH}} = 202$ Hz), 1.55–1.39 (m, 4 H, $((\text{H}_3\text{CCH}_2)(\text{CH}_3)_2\text{C})\text{PH}$), 1.13 (d, 6 H, $((\text{CH}_3)_2\text{H}_3\text{CCH}_2)_2\text{C}_2\text{PH}$, $^2J_{\text{PH}} = 10$ Hz), 1.11 (d, 6 H, $((\text{H}_3\text{CCH}_2)(\text{CH}_3)_2\text{C})_2\text{PH}$, $^2J_{\text{PH}} = 11$ Hz), 0.898 (t, 6 H, $((\text{H}_3\text{CCH}_2)(\text{CH}_3)_2\text{C})_2\text{PH}$, $^3J_{\text{HH}} = 8$ Hz). $^{13}\text{C}\{^1\text{H}\}$ NMR (C_6D_6 , 100.6 MHz): δ 36.8 (d, $((\text{H}_3\text{CCH}_2)(\text{CH}_3)_2\text{C})_2\text{PH}$, $^2J_{\text{PC}} = 14.2$ Hz), 33.8 (d, $((\text{H}_3\text{CCH}_2)(\text{CH}_3)_2\text{C})_2\text{PH}$, $^1J_{\text{PC}} = 20$ Hz), 29.4 (d, $((\text{H}_3\text{CCH}_2)(\text{CH}_3)_2\text{C})_2\text{PH}$, $^2J_{\text{PC}} = 11$ Hz), 29.0 (d, $((\text{H}_3\text{CCH}_2)(\text{CH}_3)_2\text{C})_2\text{PH}$, $^2J_{\text{PC}} = 13$ Hz), 9.529 (d, $((\text{H}_3\text{CCH}_2)(\text{CH}_3)_2\text{C})_2\text{PH}$, $^3J_{\text{PC}} = 10$ Hz). $^{31}\text{P}\{^1\text{H}\}$ NMR (C_6D_6 , 162 MHz): δ 2.9. Anal. Calcd for $\text{C}_{10}\text{H}_{23}\text{P}$: C, 68.92; H, 13.30. Found: C, 68.97; H, 13.18.

Representative Procedure for Hydrophosphination Catalysis. The compound $[\text{Ni}(\kappa^3\text{-Pigiphos})(\text{NCMeCCH}_2)](\text{ClO}_4)_2$ (**3**) [**3**] (ClO_4)₂, 0.0044 g, 2.28×10^{-6} mol) was dissolved in a mixture of acetone (1 mL) and methacrylonitrile (0.284 mL, 3.39×10^{-3} mol) to give a deep purple solution. The reaction mixture was cooled to –20 °C, and $(\text{EtMe}_2\text{C})_2\text{PH}$ (3.93×10^{-4} mol) was added. After 24 h, pentane was added to precipitate the dicationic Ni complex. The suspension was filtered, and the mother liquor was concentrated to an oil. The oil was redissolved in pentane and filtered through Al_2O_3 . Removal of volatile materials gave analytically pure $(\text{EtMe}_2\text{C})_2\text{PCH}_2\text{CHMeCN}$ (0.0815 g, 3.38×10^{-4} mol, 86%).

(Me₂EtC)₂PCH₂CHMeCN (2f). ^1H NMR (benzene-*d*₆, 500 MHz): δ 2.20 (m, 1 H, CH_2CHMeCN), 1.62 (ddd, 1 H, CH_2CHMeCN , $^2J_{\text{HH}} = 15$ Hz, $^3J_{\text{HH}} = 6.60$ Hz, $^2J_{\text{PH}} = 3$ Hz), 1.37–1.19 (m, 4 H, $\text{P}(\text{CMe}_2\text{CH}_2\text{CH}_3)_2$), 1.14 (ddd, 1 H, CH_2CHMeCN , $^2J_{\text{HH}} = 15$ Hz, $^3J_{\text{HH}} = 9$ Hz, $^2J_{\text{PH}} = 3$ Hz), 1.0 (d, 3 H, CH_2CHMeCN , $^3J_{\text{HH}} = 7$ Hz), 0.90–0.73 (m, 18 H, $\text{P}(\text{CMe}_2\text{CH}_2\text{CH}_3)_2$). $^{13}\text{C}\{^1\text{H}\}$ NMR (benzene-*d*₆, 125 MHz): δ 123.5 (d, CH_2CHMeCN , $^3J_{\text{PC}} = 9$ Hz), 35.4 (d, $\text{P}(\text{CMe}_2\text{CH}_2\text{CH}_3)_2$, $^1J_{\text{PC}} = 24$ Hz), 35.2 (d, $\text{P}(\text{CMe}_2\text{CH}_2\text{CH}_3)_2$, $^1J_{\text{PC}} = 23$ Hz), 34.6 (d, $\text{P}(\text{CMe}_2\text{CH}_2\text{CH}_3)_2$, $^2J_{\text{PC}} = 16$ Hz), 34.6 (d, $\text{P}(\text{CMe}_2\text{CH}_2\text{CH}_3)_2$, $^2J_{\text{PC}} = 16$ Hz), 26.9 (d, CH_2CHMeCN , $^2J_{\text{PC}} = 33$ Hz), 26.48 (d, CH_2CHMeCN , $^1J_{\text{PC}} = 27$ Hz), 26.3 (d, $\text{P}(\text{CMe}_2\text{CH}_2\text{CH}_3)_2$, $^2J_{\text{PC}} = 14$ Hz), 26.3 (d, $\text{P}(\text{CMe}_2\text{CH}_2\text{CH}_3)_2$, $^2J_{\text{PC}} = 14$ Hz), 25.9 (d, $\text{P}(\text{CMe}_2\text{CH}_2\text{CH}_3)_2$, $^2J_{\text{PC}} = 10$ Hz), 25.87 (d, $\text{P}(\text{CMe}_2\text{CH}_2\text{CH}_3)_2$, $^2J_{\text{PC}} = 10$ Hz), 19.9 (d, CH_2CHMeCN , $^3J_{\text{PC}} = 10$ Hz), 8.9 (d, $\text{P}(\text{CMe}_2\text{CH}_2\text{CH}_3)_2$, $^3J_{\text{PC}} = 8$ Hz), 8.8 (d, $\text{P}(\text{CMe}_2\text{CH}_2\text{CH}_3)_2$, $^3J_{\text{PC}} = 8$ Hz). $^{31}\text{P}\{^1\text{H}\}$ NMR (benzene-*d*₆, 202.5 MHz): δ 18.5. IR (neat, cm^{-1}): 2966 (s), 2239 (m), 1462 (s), 1413 (m), 1379 (s), 1364 (s), 1144 (m), 1109 (m), 1054 (m), 1008 (m), 904 (w). Anal. Calcd for $\text{C}_{14}\text{H}_{28}\text{NP}$: C, 69.67; H, 11.69; N, 5.80; Found: C, 69.43; H, 11.94; N, 5.94. $[\alpha]_D^{20} = 2.27 \pm 0.09$ (CH_2Cl_2 , $c = 1$ M) at 90% ee.

Cy₂PCEtHCH₂CN (2g). ^1H NMR (CD_2Cl_2 , 400 MHz): δ 2.59 (m, 1 H, CHCH_2CN , $^2J_{\text{HH}} = 17$ Hz), 2.43 (m, 1 H, CHCH_2CN), 1.84 (m, 1 H, CHCH_2CN), 1.77 (br m, 8 H, C_6H_{11}), 1.68–1.54 (m, 6 H, $\text{H}_3\text{CCH}_2\text{-CP}(\text{C}_6\text{H}_{11})_2$), 1.26 (br m, 10 H, C_6H_{11}), 1.06 (t, 3 H, $\text{H}_3\text{CCH}_2\text{P}$, $^3J_{\text{HH}} = 7$ Hz). $^{13}\text{C}\{^1\text{H}\}$ NMR (CD_2Cl_2 , 100 MHz): δ 119.8 (d, CN, $^3J_{\text{PC}} = 5.11$ Hz), 32.0 (*ortho*- C_6H_{11} , $^2J_{\text{PC}} = 17$ Hz), 32.0 (*ortho*- C_6H_{11} , $^2J_{\text{PC}} = 18$ Hz), 31.6 (*ipso*- C_6H_{11} , $^1J_{\text{PC}} = 35$ Hz), 31.4 (*ipso*- C_6H_{11} , $^1J_{\text{PC}} = 36$ Hz), 31.1 (*ortho*- C_6H_{11} , $^2J_{\text{PC}} = 19$ Hz), 31.0 (*ortho*- C_6H_{11} , $^2J_{\text{PC}} = 11$ Hz), 30.9 ($\text{PCH}_2\text{EtCH}_2\text{CN}$, $^1J_{\text{PC}} = 31$ Hz), 27.8 (*meta*- C_6H_{11} , $^2J_{\text{PC}} = 10$ Hz), 27.8 (*meta*- C_6H_{11} , $^2J_{\text{PC}} = 9$ Hz), 26.8 (*para*- C_6H_{11} , $^4J_{\text{PC}} = 1$ Hz), 27 (*para*- C_6H_{11} , $^4J_{\text{PC}} = 1$ Hz), 25.7 ($\text{H}_3\text{CCH}_2\text{CCHP}$, $^2J_{\text{PC}} = 12$ Hz), 20.8 (CHCH_2CN , $^2J_{\text{PC}} = 14$ Hz), 12.8 ($\text{H}_3\text{CCH}_2\text{CCHP}$, $^3J_{\text{PC}} = 9$ Hz). $^{31}\text{P}\{^1\text{H}\}$ NMR (CD_2Cl_2 , 162 MHz): δ 7.8. IR (neat oil, cm^{-1}): 2928 (s), 2851 (s), 2666 (w), 2243 (m), 1448 (s), 1423 (m), 1379 (w), 1343 (w), 1293 (w), 1269 (w), 1176 (w), 1115 (w), 1001 (m), 887 (m). Anal.

Calcd for $\text{C}_{17}\text{H}_{30}\text{NP}$: C, 73.08; H, 10.82; N, 5.01; Found: C, 73.23; H, 10.99; N, 4.93. $[\alpha]_D^{20} = 2.29 \pm 0.08$ (CH_2Cl_2 , $c = 1$ M) at 70% ee.

$[\text{Ni}((R)\text{-}(S)\text{-}\kappa^3\text{-Pigiphos})(\text{NCMeCCH}_2)](\text{ClO}_4)_2 \cdot (\text{NCMeCCH}_2) \cdot ([3]\text{-ClO}_4)_2 \cdot (\text{NCMeCCH}_2)$. **Pigiphos** (1.153 g, 1.27×10^{-3} mol) and $[\text{Ni}(\text{H}_2\text{O})_6](\text{ClO}_4)_2$ (0.464 g, 1.27×10^{-3} mol) were mixed in methacrylonitrile (3 mL) to give a purple solution. The solution was filtered, and **3** [ClO_4]₂ was crystallized by slow diffusion of OEt_2 into the methacrylonitrile solution at –20 °C. The compound was barely soluble in THF-*d*₈ and was slightly more soluble (but reacted slowly) in CD_2Cl_2 to form $[\text{Ni}(\kappa^3\text{-Pigiphos})\text{Cl}][\text{ClO}_4]$. Thus, ^1H and $^{31}\text{P}\{^1\text{H}\}$ NMR spectra were obtained in CD_2Cl_2 . Excess methacrylonitrile was required to obtain a $^{13}\text{C}\{^1\text{H}\}$ NMR spectrum, and the resulting spectrum was unfortunately obscured by the large methacrylonitrile peaks. Yield = 1.37 g (1.03×10^{-3} mol, 80.7%). ^1H NMR (THF-*d*₈): δ 8.98 (m, 5 H, $\text{P}(\text{C}_6\text{H}_5)_2$), 7.75 (br m, 1 H, $\text{P}(\text{C}_6\text{H}_5)_2$), 7.61 (br t, 5 H, $\text{P}(\text{C}_6\text{H}_5)_2$), 7.52 (br t, 5 H, $\text{P}(\text{C}_6\text{H}_5)_2$), 7.35 (br t, 3 H, $\text{P}(\text{C}_6\text{H}_5)_2$), 7.10 (br t, 1 H, $\text{P}(\text{C}_6\text{H}_5)_2$), 5.79 (s, 2 H, H_2CCMeCN), 5.75 (s, 2 H, H_2CCMeCN), 5.07 (s, 2 H, C_5H_3), 4.86 (s, 1 H, C_5H_3), 4.78 (s, 1 H, C_5H_3), 4.70 (s, 1 H, C_5H_3), 4.20 (s, 5 H, C_5H_5), 4.18 (s, 1 H, C_5H_3), 3.69 (s, 7 H, C_5H_5 and CHCH_3), 2.55 (br, 1 H, C_6H_{11}), 2.21 (m, 13 H, C_6H_{11} and CH_3), 1.95 (s, 6 H, H_2CCMeCN). $^{13}\text{C}\{^1\text{H}\}$ NMR (CD_2Cl_2 /methacrylonitrile, 100 MHz): δ 135.1 (br, **Pigiphos-Ph**), 134.0 (**Pigiphos-Ph**), 133.8 (**Pigiphos-Ph**), 133.4 (br, **Pigiphos-Ph**), 133.3 (**Pigiphos-Ph**), 132.2 (br, **Pigiphos-Ph**), 131.5 (**NC(CH}_3\text{)CCH}_2), 130.5 (br, **Pigiphos-Ph**), 130.3 (br, **Pigiphos-Ph**), 119.6 (**NC(CH}_3\text{)CCH}_2), 118.5 (**NC(CH}_3\text{)CCH}_2), 75.0 (br, **Pigiphos-C}_5\text{H}_3), 74.1 (br, **Pigiphos-C}_5\text{H}_3), 73.2 (br, **Pigiphos-C}_5\text{H}_3), 73.0 (**Pigiphos-C}_5\text{H}_3), 72.2 (**Pigiphos-C}_5\text{H}_3), 71.8 (**Pigiphos-C}_5\text{H}_3), 71.8 (br, **Pigiphos-C}_5\text{H}_3), 71.5 (br, **Pigiphos-C}_5\text{H}_3), 69.7 (**Pigiphos-C}_5\text{H}_3), 69.6 (**Pigiphos-C}_5\text{H}_3), 39.9 (**Pigiphos**), 33.3 (**Pigiphos**), 29.2 (**Pigiphos**), 27.2 (**Pigiphos**), 26.0 (**Pigiphos**), 26.0 (**Pigiphos**), 25.9 (**Pigiphos**), 20.8 (**NC(CH}_3\text{)CCH}_2), 15.3 (**Pigiphos**), 15.2 (**Pigiphos**). $^{31}\text{P}\{^1\text{H}\}$ NMR (CD_2Cl_2 , –20 °C): δ 85.8 (CyP, $^2J_{\text{PP}(\text{cis})} = 62$, 81 Hz), 19 (Ph_2P , $^2J_{\text{PP}(\text{trans})} = 208$ Hz), 8.9 (Ph_2P). IR (Nujol, cm^{-1}): 2856 (s), 2254 (m), 2224 (w), 1480 (w), 1436 (m), 1150 (w), 999 (w), 751 (m), 700 (m), 623 (m). Anal. Calcd for $\text{C}_{62}\text{H}_{67}\text{Cl}_2\text{Fe}_2\text{N}_2\text{NiO}_9\text{P}_3$: C, 56.48; H, 5.12; N, 2.12. Found: C, 56.17; H, 5.34; N, 2.31.****************************

$[\text{Ni}((R)\text{-}(S)\text{-}\kappa^3\text{-Pigiphos})\text{Br}][\text{BARf}] \cdot ([6][\text{BARf}])$. NiBr_2 (0.024 g, 1.11×10^{-4} mol) and **Pigiphos** (0.101 g, 1.11×10^{-4} mol) were stirred in THF giving a red mixture. Addition of $\text{K}[\text{BARf}]$ (0.099 g, 1.01×10^{-4} mol, $\text{BARf} = \text{tetrakis}(3,5\text{-bis}(\text{trifluoromethyl})\text{phenyl})\text{borate}$) as a solution in THF gave a homogeneous purple solution, which was stirred for 3 h. Volatiles were removed in vacuo, and the purple solid was extracted with benzene (3 \times 15 mL). The benzene solution was frozen, and lyophilization afforded $[\text{Ni}((R)\text{-}(S)\text{-}\kappa^3\text{-Pigiphos})\text{Br}][\text{BARf}]$ as a purple powder (0.190 g, 9.92×10^{-5} mol, 90.5%). ^1H NMR (toluene-*d*₈, 47 °C, 400 MHz): δ 8.29 (br s, 8 H, *ortho*- $\text{B}(\text{C}_6\text{H}_3(\text{CF}_3)_2)_4$), 7.87 (br s, 2 H, $\text{P}(\text{C}_6\text{H}_5)_2$), 7.71 (br s, 6 H, overlapping $\text{B}(\text{C}_6\text{H}_3(\text{CF}_3)_2)_4$ and $\text{P}(\text{C}_6\text{H}_5)_2$), 7.13 (br s, $\text{P}(\text{C}_6\text{H}_5)_2$), 7.08 (m, 10 H, $\text{P}(\text{C}_6\text{H}_5)_2$), 6.82 (m, 2 H, $\text{P}(\text{C}_6\text{H}_5)_2$), 4.30 (s, 1 H, C_5H_3), 4.20 (s, 1 H, C_5H_3), 4.09 (s, 2 H, C_5H_3), 3.97 (s, 1 H, C_5H_3), 3.92 (s, 1 H, C_5H_3), 3.46 (s, 5 H, C_5H_5), 3.39 (s, 5 H, C_5H_5), 3.27 (m, 1 H, $\text{PCHMeC}_5\text{H}_3\text{FeCp}$), 3.12 (m, 1 H, $\text{PCHMeC}_5\text{H}_3\text{FeCp}$), 2.36 (br s, 2 H, C_6H_{11}), 1.78 (s, 1 H, C_6H_{11}), 1.56 (q, 3 H, $\text{PCHMeC}_5\text{H}_3\text{FeCp}$), 1.46 (q, 3 H, $\text{PCHMeC}_5\text{H}_3\text{FeCp}$), 1.42 (br m, 4 H, C_6H_{11}), 1.09 (br m, 1 H, C_6H_{11}), 0.87 (q, 1 H, C_6H_{11}), 0.67 (q, 1 H, C_6H_{11}), 0.49 (br m, 1 H, C_6H_{11}). $^{13}\text{C}\{^1\text{H}\}$ NMR (toluene-*d*₈, 47 °C, 100 MHz): δ 162.70 (q, $^1J_{\text{BC}} = 50$ Hz, *ipso*- $\text{C}_6\text{H}_3(\text{CF}_3)_2$), 135.9 (t, C_6H_5), 135.6 (s, *ortho*- $\text{C}_6\text{H}_3(\text{CF}_3)_2$), 135.3 (t, C_6H_5), 134.6 (t, C_6H_5), 134.2 (br t, C_6H_5), 132.1 (s, C_6H_5), 131.6 (s, C_6H_5), 131.0 (d, C_6H_5), 130.5 (br m, C_6H_5), 130.1 (q, C_6H_5), 129.8 (q, C_6H_5), 129.5 (m, C_6H_5), 129.5 (s, C_6H_5), 128.7 (m, *meta*- $\text{C}_6\text{H}_3(\text{CF}_3)_2$), 128.4 (m, C_6H_5), 125.6 (q, $\text{C}_6\text{H}_3(\text{CF}_3)_2$), 124.1 (s, C_6H_5), 121.3 (s, C_6H_5), 118.0 (s, *para*- $\text{C}_6\text{H}_3(\text{CF}_3)_2$), 92.5 (br, C_5H_3), 89.7 (br, C_5H_3), 75.0 (s, C_5H_3), 74.6 (s, C_5H_3), 71.4 (s, C_5H_5), 71.3 (s, C_5H_3), 70.7 (s, C_5H_3), 70.4 (s, 2 C, C_5H_3), 69.2 (s, C_5H_3), 38.1 (d, $^1J_{\text{PC}} = 17$ Hz, C_6H_{11}), 32.0 (d, $^1J_{\text{PC}} = 15$ Hz, $\text{PCHMeC}_5\text{H}_3\text{FeCp}$), 30.6 (br, $\text{PCHMeC}_5\text{H}_3\text{FeCp}$), 30.5 (bf, C_6H_{11}), 28.7 (s, C_6H_{11}), 26.4 (d, $^2J_{\text{PC}} = 10$ Hz, C_6H_{11}), 25.8 (d, $^2J_{\text{PC}} = 11$ Hz, C_6H_{11}),

25.4 (s, C_6H_{11}), 19.4 (br $PCHMeC_5H_3FeCp$), 14.9 (d, $^2J_{PC} = 8.85$ Hz, $PCHMeC_5H_3FeCp$). $^{31}P\{^1H\}$ (toluene- d_8 , -40 °C, 162 MHz): δ 78.1 (br virtual t, CyP-minor conformer), 74.8 (virtual t, CyP, major conformer), 14.0 (dd, $^2J_{PP(trans)} = 286$ Hz, $^2J_{PP(cis)} = 59$ Hz, minor conformer, PPh_2), 13.05 (dd, $^2J_{PP(cis)} = 63$ Hz, PPh_2), 11.5 (br s, PPh_2), 3.9 (dd, $^2J_{PP(trans)} = 301$ Hz, $^2J_{PP(cis)} = 69$ Hz, PPh_2). ^{11}B NMR (toluene- d_8 , 96.3 MHz): δ -6 . ^{19}F NMR (toluene- d_8 , 188.3 MHz): δ -62 . IR (Nujol, cm^{-1}): 2955 (s), 1610 (w), 1461 (m), 1437 (m), 1355 (s), 1001 (w), 887 (m). Anal. Calcd. for $C_{86}H_{67}BBBrF_{24}FeNiP_3$: C, 54.07; H, 3.53; Found: C, 53.81; H, 3.75.

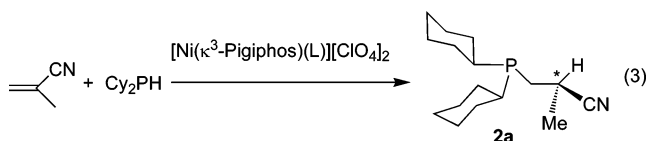
Kinetics Measurements. Reactions were monitored by 1H NMR spectroscopy with a Bruker DRX400 spectrometer. The catalyst $[3][BARf]_2$ was dissolved in a stock solution of methacrylonitrile (3.20 M) and 1,3,5-trimethoxybenzene (0.076 M) in toluene- d_8 . Immediately before data acquisition, t -Bu $_2$ PH was added by syringe through a septum, and the NMR tube was shaken and placed in the preshimmed and preheated NMR spectrometer. Single-scan spectra were acquired automatically at preset time intervals (3 min). The peaks were integrated relative to the known concentration of 1,3,5-trimethoxybenzene as an internal standard. A nonweighted linear least-squares fit of the integrated second-order rate law $\ln\{[\text{methacrylonitrile}]_t/[t\text{-Bu}_2\text{PH}]_t\} = \ln\{[\text{methacrylonitrile}]_0/[t\text{-Bu}_2\text{PH}]_0\} + k\Delta t$ was used to determine rate constants.²² The isotope effect was determined by comparing k_{obs} for t -Bu $_2$ PH and t -Bu $_2$ PD with an identical sample of $[3][BARf]_2$ as the catalyst in separate experiments.

DFT Methods. Geometries and energies of all reactants, intermediates, transition states, and products have been calculated using B3LYP level density functional theory using the Gaussian-03 package.²³ The basis set lanl2dz was used for nickel,²⁴ 6-311+G(d) for phosphorus, and 6-311G for nitrogen, carbon and hydrogen.²⁵ Normal-mode analyses were performed on all optimized structures, and zero-point energy (ZPE) and Gibbs free energy corrections have been applied at 298.15 K. Minima contain zero negative-frequency modes, and transition states are characterized by exactly one negative frequency, corresponding to a first-order saddle point on the potential energy surface.

Results

Catalytic Enantioselective Hydrophosphination of Methacrylonitrile. Initial hydrophosphination experiments were performed under conditions optimized for our Ni-catalyzed asymmetric hydroamination of methacrylonitrile.¹⁶ Reaction of Cy $_2$ PH and methacrylonitrile in THF (2 equiv of methacrylonitrile, 5 mol % of $[1][ClO_4]_2$ relative to Cy $_2$ PH) gives a new product after 1 h at r.t., as determined by $^{31}P\{^1H\}$ NMR spectroscopy (-8.12 ppm) and GC-MS analysis (265 amu). However, these conditions do not afford good conversion for this hydrophosphination even after extended reaction times, and a higher catalyst loading (20 mol %) does not provide significantly enhanced rates or yield. A possible explanation for the catalyst's inactivity is that coordination of Cy $_2$ PH and/or the tertiary phosphine product to the Ni center gives a substitutionally inert species. To favor the coordination of methacrylonitrile and establish catalytic hydrophosphination, methacrylonitrile was employed as both solvent and substrate.

In methacrylonitrile, Cy $_2$ PH reacts in the presence of 10 mol % of $[1][ClO_4]_2$ to quantitatively form Cy $_2$ PCH $_2$ CHMeCN (**2a**) after 1 h (eq 3). The product **2a** is easily isolated by addition of



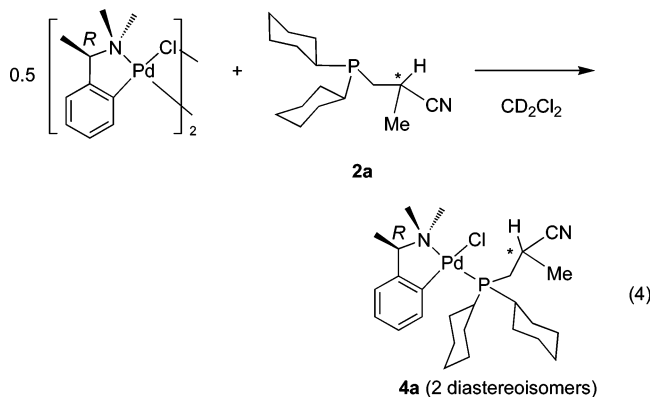
pentane to the reaction mixture followed by filtration through Al_2O_3 under a N_2 atmosphere.

Characterization of **2a** indicated that it is the anti-Markovnikov addition product, as determined by three multiplets in its 1H NMR spectrum from the methine hydrogen (2.18 ppm) and two diastereotopic methylene hydrogens (1.48 and 1.44 ppm).

The catalyst may be the isolated $[1][ClO_4]_2$ or generated in situ by mixing $[Ni(H_2O)_6][ClO_4]_2$ and Pigiphos in methacrylonitrile. 1H and $^{31}P\{^1H\}$ NMR spectra of this mixture and of $[1][ClO_4]_2$ /methacrylonitrile mixtures are identical and indicate that the only Pigiphos-containing species in solution is $[Ni(\kappa^3\text{-Pigiphos})(NCMeCCH_2)][ClO_4]_2$ (**3**) ($[3][ClO_4]_2$, vide infra). Apparently, the presence or absence of small amounts of water does not interfere with the formation of **3** or inhibit the catalytic hydrophosphination reaction.

Racemic mixtures of **2a** initially proved difficult to prepare via conventional methods, possibly because vinyl nitriles are relatively unreactive in 1,4-addition reactions.²⁶ Although conditions for the preparation of related acrylonitrile–phosphine adducts $PH_n(CH_2CH_2CN)_{3-n}$ involving radical- and base-promoted reactions have been reported,^{5,6} the best method for preparing the racemic form of our catalytic asymmetric hydrophosphination products uses F_3CCH_2OH as the solvent and catalyst. Additionally, several (achiral) transition-metal-catalyzed hydrophosphinations were attempted; the difficulties associated with these reactions highlight the unique advantage of our Ni(II)-(Pigiphos) system. For example, in methacrylonitrile as solvent, the Ni salt $[Ni(H_2O)_6][ClO_4]_2$ itself promotes the addition of Cy $_2$ PH to methacrylonitrile, but the phosphine product coordinates to Ni and is difficult to isolate. In contrast, mixtures of another common tris-chelating phosphine Triphos (Triphos = tris(diphenylphosphinomethyl)ethane) and $[Ni(H_2O)_6][ClO_4]_2$ in methacrylonitrile do not afford detectable quantities of **2a**. Although methacrylonitrile and Cy $_2$ PH react in the presence of 10 mol % of $[Pt(norbornene)_3]$ in toluene at 100 °C to give racemic **2a**,⁷ the bulkier secondary phosphines t -Bu $_2$ PH and (1-Ad) $_2$ PH produce only traces of addition products.

The enantiomeric excess was determined by reaction of **2a** and an enantiopure palladium complex $[(R\text{-}\kappa^2\text{-}C_6H_4CHMeNMe_2)\text{-}Pd(\mu\text{-}Cl)_2]$ to give $[(R\text{-}\kappa^2\text{-}C_6H_4CHMeNMe_2)Pd(Cy_2PCH_2CHMeCN)Cl]$ (**4a**) in methylene chloride- d_2 (eq 4).^{20,27} The $^{31}P\{^1H\}$



- (22) Espenson, J. H. *Chemical Kinetics and Reaction Mechanisms*, 2nd ed.; McGraw-Hill: New York, 1995; p 155.
 (23) (a) Frisch, M. J.; et al. *Gaussian 03*; Gaussian, Inc.: Wallingford, CT, 2004. (b) Becke, A. D. *J. Chem. Phys.* **1993**, *98*, 5648–5652.
 (24) (a) Hay, P. J.; Wadt, W. R. *J. Chem. Phys.* **1985**, *82*, 270–283. (b) Hay, P. J.; Wadt, W. R. *J. Chem. Phys.* **1985**, *82*, 299–310.
 (25) (a) McLean, A. D.; Chandler, G. S. *J. Chem. Phys.* **1980**, *72*, 5639–5648. (b) Krishnan, R.; Binkley, J. S.; Seeger, R.; Pople, J. A. *J. Chem. Phys.* **1980**, *72*, 650–654.

Table 1. $[\text{Ni}(\kappa^3\text{-Pigiphos})(\text{THF})]^{2+}$ -Catalyzed Hydrophosphination Reactions of R_2PH in Methacrylonitrile

entry	Phosphine	Product	turnover	% ee
1	Cy_2PH		10	65
2	Ph_2PH		10	18
3	$i\text{-Pr}_2\text{PH}$		10	n.d.
4	$t\text{-Bu}_2\text{P}$		100	65
5	$(1\text{-Ad})_2\text{PH}$		20	80

NMR spectrum of this reaction mixture displayed two separated signals for the two diastereomeric complexes, and the enantiomeric excess was calculated from the relative integrated intensities of the two resonances.⁹

With the use of the conditions mentioned, reactions of methacrylonitrile and a series of secondary phosphines were examined (Table 1). The progress of the hydrophosphination reactions is conveniently monitored by $^3\text{P}\{^1\text{H}\}$ NMR spectroscopy, and the products are identified by the characteristic methine signal in their ^1H NMR spectra and their mass spectrum from GC-MS analysis. Thus, diphenylphosphine and methacrylonitrile react in the presence of the in situ-generated catalyst to give $\text{Ph}_2\text{PCH}_2\text{CHMeCN}$ (**2b**; $^3\text{P}\{^1\text{H}\}$ NMR: -19.0 ppm). Isolation of **2b** proved more difficult than for **2a** due to its insolubility in hexane, and as a result the isolated yield of **2b** is low. Mes_2PH does not give any conversion under these reaction conditions even after 2 weeks.

$i\text{-Pr}_2\text{PH}$ reacts in methacrylonitrile in the presence of 10 mol % of catalyst to give $i\text{-Pr}_2\text{PCH}_2\text{CHMeCN}$ (**2c**) with complete conversion ($^3\text{P}\{^1\text{H}\}$ NMR: 0.98 ppm). However, when additional $i\text{-Pr}_2\text{PH}$ was added to the reaction mixture, conversion was slow and incomplete even after 1 week, thus indicating catalyst deactivation. Interestingly, sterically hindered secondary phosphines permit lower catalyst loadings. For example, $t\text{-Bu}_2\text{PH}$ reacts in methacrylonitrile with 1 mol % of catalyst to give complete conversion to $t\text{-Bu}_2\text{PCH}_2\text{CHMeCN}$ (**2d**) after 1 day ($^3\text{P}\{^1\text{H}\}$ NMR: 23.2 ppm). $(1\text{-Ad})_2\text{PH}$ (20 equiv) reacts in methacrylonitrile in the presence of $[\text{I}][\text{ClO}_4]_2$ to quantitatively form $(1\text{-Ad})_2\text{PCH}_2\text{CHMeCN}$ (**2e**) after 20 min ($^3\text{P}\{^1\text{H}\}$ NMR: 19.7 ppm). Although $(1\text{-Ad})_2\text{PH}$ is partially insoluble in the reaction mixture, conversion proceeds readily. The enantioselectivities of these reactions were again evaluated by $^3\text{P}\{^1\text{H}\}$ NMR spectroscopy, but in this case the $^3\text{P}\{^1\text{H}\}$ NMR signals of the two palladium diastereoisomers were poorly resolved. Therefore, the products **2d** and **2e** were oxidized to the corresponding phosphine oxides and mixed with the chiral

Table 2. Effect of Counterion, Temperature, and Solvent on Enantioselectivity in the Formation of $t\text{-Bu}_2\text{PCH}_2\text{CHMeCN}$ Catalyzed by $[\text{Ni}(\kappa^3\text{-Pigiphos})(\text{L})]^{2+}$

entry	counteranions	T ($^\circ\text{C}$)	time	solvent	turnover no.	ee (%)
1	$[\text{ClO}_4]_2$	25	24 h	methacrylonitrile	98	65
2	$[\text{ClO}_4]_2$	25	216 h	$\text{THF-}d_8$	46	n.d.
3	$[\text{ClO}_4]_2$	25	10 min	$\text{F}_3\text{CCH}_2\text{OH}$	113	46
4	$[\text{ClO}_4]_2$	25	1 h	acetone	38	77
5	$[\text{BF}_4]_2$	25	3 h	acetone- d_6	55	50
6	$[\text{BPh}_4]_2$	25	48 h	$\text{THF-}d_8$	121	67
7	$[\text{BF}_4]_2$	-78 to 25	12 h	acetone	46	84
8	$[\text{ClO}_4]_2$	-78 to 25	12 h	acetone	112	84
9	$[\text{BArf}]_2$	-20	24 h	toluene	300	71
10	$[\text{ClO}_4]_2$	-20	24 h	acetone	100	89
11	$[\text{BArf}]_2$	-20	168 h	acetone	92	75
12	$[\text{OTf}]_2$	-20	140 h	acetone	65	65
13	$[\text{BArf}][\text{OTf}]$	-20	48 h	acetone	85	72

shift reagent tris(3-trifluoromethylhydroxymethylene-*d*-camphorate)europium to give two well-resolved signals.²⁸

Of this series of phosphines, the bulky secondary phosphine $t\text{-Bu}_2\text{PH}$ gives the best results in terms of conversion and enantioselectivity, and its reaction with methacrylonitrile is conveniently monitored by ^1H and $^3\text{P}\{^1\text{H}\}$ NMR spectroscopy. Therefore, our efforts to further develop this hydrophosphination process focused on $t\text{-Bu}_2\text{PH}$. In a series of experiments, the effects of different counterions, solvents, and temperature on the conversion, rate, and enantioselectivity were investigated (see Table 2). Polar solvents, such as acetone and $\text{F}_3\text{CCH}_2\text{OH}$, were initially chosen for their ability to dissolve the salt $[\text{I}][\text{ClO}_4]_2$. Under catalytic conditions with excess methacrylonitrile, the Ni catalyst is partially soluble in THF or methacrylonitrile, but there is always some undissolved solid in the reactions mixture. The solvent $\text{F}_3\text{CCH}_2\text{OH}$ solubilizes the catalyst much better, and increased rates are observed in that solvent compared to THF (cf. entries 2 and 3). The compound $[\text{Ni}(\kappa^3\text{-Pigiphos})(\text{NCMeC}=\text{CH}_2)][\text{BPh}_4]_2$ (**3**) $[\text{BPh}_4]_2$; vide infra) is more soluble in THF, and a higher conversion results, but the reaction is still relatively slow (entry 6). Hydrophosphination is possible in toluene when a more soluble complex such as $[\text{Ni}(\kappa^3\text{-Pigiphos})(\text{NCMeC}=\text{CH}_2)][\text{BArf}]_2$ (**3**) $[\text{BArf}]_2$; vide infra) is the catalyst. Comparison of the enantioselectivities of the reaction of $t\text{-Bu}_2\text{PH}$ and methacrylonitrile in these different solvents reveals that at r.t. acetone gives the best selectivity (entry 4, 77% ee). Although $\text{F}_3\text{CCH}_2\text{OH}$ itself catalyzes the reaction of $t\text{-Bu}_2\text{PH}$ and methacrylonitrile, this background reaction (>1 day at r.t.) is much slower than the catalytic reaction (10 min). In contrast, $t\text{-Bu}_2\text{PH}$ and methacrylonitrile do not react in acetone, THF, or methacrylonitrile in the absence of the Ni catalyst.

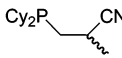
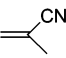
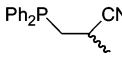
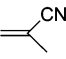
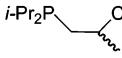
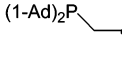
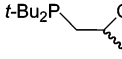
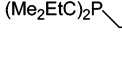
Despite the solubility problems of **3** $[\text{ClO}_4]_2$, catalysts with the ClO_4^- counterion provide the best enantioselectivity (cf. entries 4 vs 5 and 9–12). For example, direct comparison of **3**²⁺ complexes with BF_4^- and ClO_4^- as counterions (entries 4 and 5) shows substantially increased ee's for reactions with the perchlorate. The catalysts containing the less-coordinating counterion $[\text{BArf}]^-$ affords the product in lower enantiomeric excess in comparison to those with ClO_4^- . Interestingly, successive replacement of $[\text{BArf}]^-$ with TfO^- as the counterion results in lower enantioselectivity. The selectivity trends ob-

(26) Fleming, F. F.; Wang, Q. *Chem. Rev.* **2003**, *103*, 2035–2077.

(27) Determination of the enantiomeric excess by chiral HPLC and GC was hampered by a slow oxidation process, and attempts to resolve stable derivatives such as phosphine sulfides and oxides by chiral HPLC and GC on OD-H and OJ cellulose columns were unsuccessful. Thus, NMR appears to be the best method for determining the % ee of the 2-cyanopropyl phosphine products.

(28) McCreary, M. D.; Lewis, D. W.; Wernick, D. L.; Whitesides, G. M. *J. Am. Chem. Soc.* **1974**, *96*, 1038–1054.

Table 3. Optimized Conditions for the Addition of R₂PH to Methacrylonitrile Catalyzed by [Ni(κ³-Pigiphos)(L)][ClO₄]₂

entry	R ₂ PH	product	turnover number	Solvent	yield ^a (%)	% ee
1	Cy ₂ PH		10		71	70
2	Ph ₂ PH		15		10	32
3	<i>i</i> -Pr ₂ PH		49	acetone	not isolated	78
4	(1-Ad) ₂ PH		100	acetone	95	94
5	<i>t</i> -Bu ₂ PH		100	acetone	97	89
6	(EtMe ₂ C) ₂ PH		116	acetone	86	90

^a Isolated yield, based on R₂PH.

served at r.t. are maintained at lower temperature, and accordingly the best enantioselectivities are obtained in acetone with [3][ClO₄]₂ at −20 °C. Reaction rates at lower temperature (less than −20 °C) are significantly decreased.

Hydrophosphination was attempted with a few other vinyl nitriles. Although the vinyl nitrile *cis*-2-pentenitrile and *t*-Bu₂PH do not react (2 weeks, r.t., as reagent and solvent), Cy₂PH reacts in the presence of [1][ClO₄]₂ to give Cy₂P(Et)-HCCH₂CN (**2g**; 24 h, r.t.). Unfortunately, the enantiomeric excess is low (24%). Note that the position of the stereogenic carbon in **2g** is different than in the products of methacrylonitrile hydrophosphination (β rather than α carbon). Neither *trans*-cinnamonitrile nor cyclohexenecarbonitrile gave hydrophosphination products under our catalytic conditions with R₂PH (R = Ph, Cy, *t*-Bu; 1–10% catalyst, neat vinyl nitrile) (see Table 3).

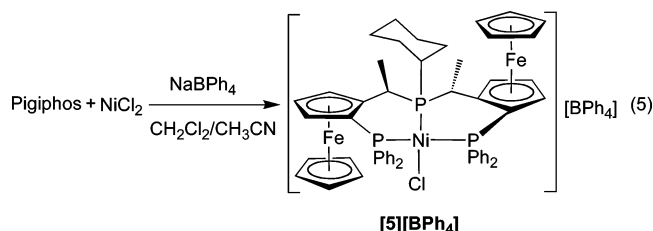
Absolute Configuration of Hydrophosphination Products. The absolute configurations of the products *t*-Bu₂PCH₂-CHMeCN and (1-Ad)₂PCH₂CHMeCN were determined by single-crystal X-ray diffraction of their coordination complexes with the cyclometalated Pd derivative of (1*R*)-*N,N*-dimethyl-1-(1-naphthyl)ethylamine.²¹ The X-ray structures reveal that the major isomer of our hydrophosphination, both with *t*-Bu₂PH and (1-Ad)₂PH, has *S* absolute configuration, whereas the corresponding [1][ClO₄]₂-catalyzed hydroaminations give *R* configured products. However, note that for the two different types of products the priority sequence of the compounds' substituents is different. Therefore, it can be said that Ni catalysts containing Pigiphos of the (*R*)-(*S*) absolute configuration catalyze the addition of both secondary amines and phosphines across the *si*-side of methacrylonitrile preferentially.

Synthesis of [Ni(Pigiphos)(methacrylonitrile)][A]₂ (A = ClO₄, BF₄, BPh₄, BARf) and [Ni(Pigiphos)X][A] (X = Cl, A = BPh₄; X = Br, A = BARf). The compounds [Ni(H₂O)₆][ClO₄]₂ and Pigiphos react in methacrylonitrile to produce a deep purple solution of [Ni(κ³-Pigiphos)(NCMeCCH₂)] [ClO₄]₂ ([3][ClO₄]₂) that crystallizes upon standing. This compound is soluble in methylene chloride, but unfortunately reacts to give [Ni(κ³-Pigiphos)Cl][ClO₄] within ca. 2 h. Isolated [3][ClO₄]₂ is only slightly soluble in THF and completely insoluble in benzene, hexane, and Et₂O. ¹H and ³¹P{¹H} NMR spectra

(CD₂Cl₂) show two inequivalent diphenylphosphinoferrocene moieties, as is observed for the noncoordinated Pigiphos ligand and a series of Ni(II)(Pigiphos) compounds [Ni(κ³-Pigiphos)X][A] (X = Cl, Br; A = PF₆, ClO₄, BF₄, BPh₄, B(C₆H₃(CF₃)₂)₄). Additionally, integration of the ¹H NMR spectrum indicated that there are two molecules of methacrylonitrile associated with one [Ni(κ³-Pigiphos)]²⁺, which are equivalent on the ¹H NMR time scale at r.t. The ³¹P{¹H} NMR spectrum (CD₂Cl₂, r.t.) contains three broad resonances which sharpen at −20 °C to two sets of resonances corresponding to two conformers in a ratio of approximately 20 to 1. Each conformer gives rise to three phosphorus resonances, which are doublets of doublets due to *cis* and *trans* ²J_{PP} couplings (major conformer: CyP, 85.77 ppm, ²J_{PP(cis)} = 61.52 and 81.45 Hz; Ph₂P, 18.96 and 8.91 ppm, ²J_{PP(trans)} = 207.92 Hz; minor conformer, ca. 5%: 77.82, 17.8, and 10.9 ppm, mostly obscured by the major conformer). The ³¹P{¹H} NMR spectrum of [3][ClO₄]₂ is similar to that of [Ni(κ³-Pigiphos)(NCCH₃)] [ClO₄]₂ (83.42, 18.10, 9.23 ppm), in which the acetonitrile is bonded to nickel via an η¹-coordination mode through its nitrogen.^{17a} The dynamic process responsible for the broad ³¹P{¹H} NMR spectrum at r.t. appears to result from two rapidly exchanging conformations of the ferrocenylethyl backbone of the Pigiphos ligands.^{17d} Similar ³¹P NMR spectra were observed for Pigiphos complexes of Ni(II), Pd(II), and Ir(I), including [Ni(κ³-Pigiphos)Br][BARf], [Pd(κ³-Pigiphos)Cl][PF₆], [Ir(κ³-Pigiphos)Cl].¹⁷ Unfortunately, detailed solution-state NMR characterization of [3][ClO₄]₂ proved to be impossible due to its insolubility and its reactivity with methylene chloride. Therefore, we sought derivatives of dicationic Ni(II)(Pigiphos) complexes containing counterions such as [BPh₄][−] and [BARf][−] leading to higher solubilities.

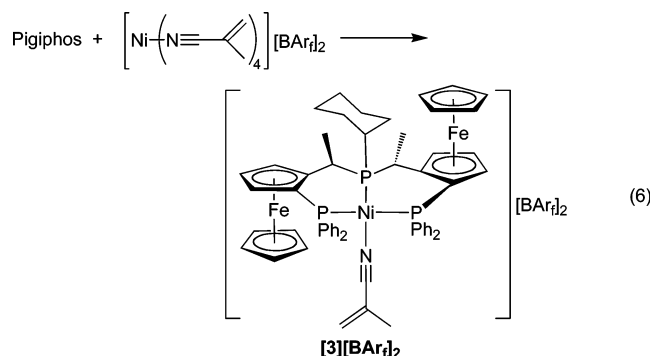
Thus, reaction of Pigiphos, NiCl₂, NaBPh₄ in methylene chloride/acetonitrile gives a purple solution (eq 5). After Soxhlet extraction with methylene chloride, [Ni(κ³-Pigiphos)Cl][BPh₄] ([5][BPh₄]) is isolated as a purple air-stable powder.

The ¹H NMR spectrum of the cationic portion [5]⁺ in CD₂Cl₂ is identical to that of [Ni(κ³-Pigiphos)Cl]⁺ containing the BF₄[−], ClO₄[−], and PF₆[−] counterions.^{16,17} Unfortunately, this compound does not react in the presence of AgBPh₄ (THF-*d*₈ or acetonitrile-*d*₃, r.t., 24 h). Compound [5][BPh₄] is also unreactive



toward potassium hexamethylsilazide, lithium morpholide, lithium diphenylamide, and potassium benzylnitrile (THF-*d*₈, r.t., 24 h). Although **[5][BPh₄]** readily dissolves in methylene chloride, its limited solubility in THF may also impair its reactivity.

We expected that nickel bromide compounds containing the $[\text{BAr}_f]^-$ anion might be more soluble and more reactive than **[5][BPh₄]**. Two synthetic routes allowed for the preparation of **[3][BAr_f]₂**. In the first, reaction of Pigiphos and $[\text{Ni}(\text{NCMeCCH}_2)_4][\text{BAr}_f]_2$ in methacrylonitrile or methacrylonitrile/toluene mixtures affords **[3][BAr_f]₂** (eq 6). This reaction



also proved useful for the preparation of $[\text{Ni}(\kappa^3\text{-Pigiphos})(\text{NCMeCCH}_2)_2][\text{BPh}_4]_2$ (**[3][BPh₄]₂**). $[\text{Ni}(\text{NCMeCCH}_2)_4][\text{A}]_2$ ($\text{A} = \text{BPh}_4, \text{BAr}_f$) is synthesized by reaction of NiBr_2 and 2 equiv of $[\text{Ag}][\text{BAr}_f]$ in methacrylonitrile, in analogy to the preparation of $[\text{Ni}(\text{NCMe})_4][\text{BAr}_f]_2$.²⁹

The compound **[3][BAr_f]₂** can also be prepared via a two-step sequence: the reaction of NiBr_2 , Pigiphos, and $[\text{K}][\text{BAr}_f]$ in THF forms $[\text{Ni}(\kappa^3\text{-Pigiphos})\text{Br}][\text{BAr}_f]$ (**[6][BAr_f]**). The reaction of this intermediate with $[\text{Ag}][\text{BAr}_f]$ in a mixture of methacrylonitrile and benzene (1:4) gives **[3][BAr_f]₂**. The $^{31}\text{P}\{^1\text{H}\}$ NMR spectra of the dication of **[3][BAr_f]₂** and **[3][BPh₄]₂** are identical to that of **[3][ClO₄]₂**. Unfortunately, signals from the Pigiphos and methacrylonitrile ligands in the ^1H NMR spectra remained broad at low temperature. Apparently, the coordinated and free methacrylonitrile are exchanging rapidly at r.t. and on the ^1H NMR time scale at -80°C .

X-ray Crystal Structures of $[\text{Ni}(\kappa^3\text{-Pigiphos})(\text{NCMeC=CH}_2)][\text{ClO}_4]_2$ ([3][ClO₄]₂**) and $[\text{Ni}(\kappa^3\text{-Pigiphos})(\text{NCHC=CH}_2)][\text{ClO}_4]_2$ (**[7][ClO₄]₂**).** X-ray quality crystals of **[3][ClO₄]₂** were grown at r.t. from a saturated methacrylonitrile solution, and the solid-state structure was determined by X-ray crystallography. The asymmetric unit contains the dicationic fragment of **[3]²⁺** (Figure 1), two ClO_4^- counterions, and an additional methacrylonitrile molecule. Selected bond distances and angles are found in Tables 4 and 5, along with corresponding values for the *cis*-2-pentenitrile derivative $[\text{Ni}(\kappa^3\text{-Pigiphos})(\text{NCHC=CH}_2)][\text{ClO}_4]_2$ (**[7][ClO₄]₂**). In **[3]²⁺**, the Ni center is coordinated by three phosphorus atoms and the methacrylonitrile nitrogen in a distorted square-planar configuration such that the Ni atom is located 0.33 Å from the plane defined by the three phosphorus atoms. The nitrile nitrogen (N1) and carbon (C15) atoms are further displaced from this plane (in the same direction) by 1.149 and 1.887 Å, respectively. This distortion is also illustrated by the angles formed by the Ni center and its sets of trans ligands, i.e., P1–Ni1–P3 and P2–Ni1–N1, which are significantly lower than 180° (160.15(3) and 163.05(9)°, respectively). The compound $[\text{Pd}(\kappa^3\text{-Pigiphos})\text{Cl}][\text{ClO}_4]$ (**[4][ClO₄]**) was also prepared by reaction of PdCl_2 and Pigiphos in THF. The structure of **[4][ClO₄]** is shown in Figure 2. The asymmetric unit contains the monocationic fragment of **[4]⁺**, one ClO_4^- counterion, and one additional methacrylonitrile molecule. Selected bond distances and angles are found in Tables 6 and 7, along with corresponding values for the *cis*-2-pentenitrile derivative $[\text{Pd}(\kappa^3\text{-Pigiphos})\text{Cl}][\text{ClO}_4]$ (**[8][ClO₄]**).

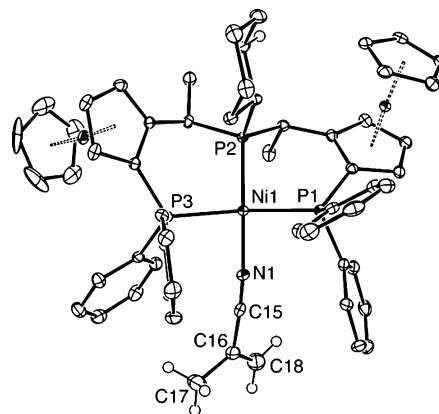


Figure 1. ORTEP diagram of the dicationic fragment of $[\text{Ni}(\kappa^3\text{-Pigiphos})(\text{NCMeC=CH}_2)][\text{ClO}_4]_2 \cdot (\text{NCMeC=CH}_2)$ (**[3][ClO₄]₂·(NCMeC=CH₂)**) illustrating the NiL_4 square plane (hydrogen atoms on Pigiphos are omitted for clarity; 30% probability ellipsoids).

Table 4. Selected Bond Lengths (Å) for $[\text{Ni}(\kappa^3\text{-Pigiphos})(\text{NC(Me)C=CH}_2)][\text{ClO}_4]_2(\text{NC(Me)C=CH}_2)$ (**[3][ClO₄]₂**) and $[\text{Ni}(\kappa^3\text{-Pigiphos})(\text{NC(H)C=CH}_2)][\text{ClO}_4]_2(\text{NC(H)C=CH}_2)$ (**[7][ClO₄]₂**)

bond length	[3][ClO₄]₂	[7][ClO₄]₂
Ni1–N1	1.879(2)	1.866(6)
Ni1–P1	2.2300(12)	2.2510(18)
Ni1–P2	2.1757(12)	2.1754(17)
Ni1–P3	2.2390(14)	2.2364(18)
N1–C15	1.133(4)	1.142(8)
C15–C16	1.445(4)	1.434(10)
C16–C17	1.502(5)	1.322(11)
C16–C18	1.307(5)	
C17–C18		1.477 (12)

Table 5. Selected Bond Angles (deg) for $[\text{Ni}(\kappa^3\text{-Pigiphos})(\text{NC(Me)C=CH}_2)][\text{ClO}_4]_2(\text{NC(Me)C=CH}_2)$ (**[3][ClO₄]₂**) and $[\text{Ni}(\kappa^3\text{-Pigiphos})(\text{NC(H)C=CH}_2)][\text{ClO}_4]_2(\text{NC(H)C=CH}_2)$ (**[7][ClO₄]₂**)^a

angle	[3][ClO₄]₂	[7][ClO₄]₂
N1–Ni1–P2	163.05(9)	173.3(2)
N1–Ni1–P1	91.40(8)	85.10(16)
N1–Ni1–P3	87.08(8)	89.12(17)
P2–Ni1–P1	91.22(3)	96.26(7)
P2–Ni1–P3	95.99(3)	91.14(7)
P1–Ni1–P3	160.15(3)	164.46(8)
N1–N1–C15	164.4(3)	177.0(6)
N1–C15–C16	176.0(3)	179.0(8)
C25–P1–C31	105.66(13)	
C37–P3–C43	105.42(13)	
C38–P1–C44		105.9(3)
C26–P3–C32		106.8(3)

^a Note that the numbering schemes for **[3]²⁺** and **[7]²⁺** are not fully identical.

$[\text{Ni}(\kappa^3\text{-Pigiphos})(\text{NCHC=CH}_2)][\text{ClO}_4]_2$ (**[7][ClO₄]₂**). In **[3]²⁺**, the Ni center is coordinated by three phosphorus atoms and the methacrylonitrile nitrogen in a distorted square-planar configuration such that the Ni atom is located 0.33 Å from the plane defined by the three phosphorus atoms. The nitrile nitrogen (N1) and carbon (C15) atoms are further displaced from this plane (in the same direction) by 1.149 and 1.887 Å, respectively. This distortion is also illustrated by the angles formed by the Ni center and its sets of trans ligands, i.e., P1–Ni1–P3 and P2–Ni1–N1, which are significantly lower than 180° (160.15(3) and 163.05(9)°, respectively). The compound $[\text{Pd}(\kappa^3\text{-Pigiphos})\text{Cl}][\text{ClO}_4]$ (**[4][ClO₄]**) was also prepared by reaction of PdCl_2 and Pigiphos in THF. The structure of **[4][ClO₄]** is shown in Figure 2. The asymmetric unit contains the monocationic fragment of **[4]⁺**, one ClO_4^- counterion, and one additional methacrylonitrile molecule. Selected bond distances and angles are found in Tables 6 and 7, along with corresponding values for the *cis*-2-pentenitrile derivative $[\text{Pd}(\kappa^3\text{-Pigiphos})\text{Cl}][\text{ClO}_4]$ (**[8][ClO₄]**).

(29) Buschmann, W. E.; Miller, J. S.; Bowman-James, K.; Miller, C. N. *Inorg. Synth.* **2002**, 33, 83–91.

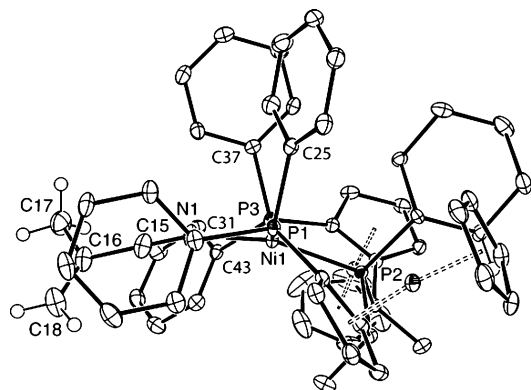


Figure 2. ORTEP diagram of the dication $[\text{Ni}(\kappa^3\text{-Pigiphos})(\text{NCMeCCH}_2)]^{2+}$ ($[3]^{2+}$), viewed down the P3–Ni1–P1 vector. The syn pseudoequatorial phenyl groups sandwich the methacrylonitrile and, together with the syn pseudoaxial phenyl substituent, create an asymmetric pocket (hydrogen atoms of Pigiphos are omitted for clarity; 30% probability ellipsoids).

$[\text{PF}_6]$ possesses a similarly distorted square-planar geometry, although the degree of distortion in $[3][\text{ClO}_4]_2$ is more severe.¹⁷

Tridentate coordination of Pigiphos to the Ni center assembles a structure containing two fused six-membered rings. The substituents' arrangement on these metallacycles, particularly the phenyl groups, is key to the asymmetric environment of Ni and its reactive site. The orientation of the Ph_2P groups, which are primarily responsible for transmitting the ligand's chiral information to coordinated substrates, displays approximate C_2 symmetry (the pseudo- C_2 axis is coincident with the Ni–P2 bond vector; note that the cyclohexyl phosphino group eliminates the possibility of true C_2 symmetry and Pigiphos is C_1 symmetric). However, the distortion described above results in a displacement of the methacrylonitrile ligand from this pseudo- C_2 axis and places it in close proximity to two phenyl groups of Pigiphos. A view along the P1–Ni1–P3 axis (Figure 2) reveals that a phenyl group from each diphenylphosphine “sandwich” the methacrylonitrile ligand. The relative position of these two phenyl groups is pseudoequatorial with respect to the fused metallabicyclic system and syn with respect to each other (necessarily, the other pair of phenyl groups are pseudoaxial and also syn). As a result, the two open axial coordination sites on the Ni are inequivalent and the methacrylonitrile ligand is situated in an unusual top/bottom asymmetric pocket.

A second vinyl nitrile complex was prepared for comparison with $[3][\text{ClO}_4]_2$. Reaction of $[\text{Ni}(\text{H}_2\text{O})_6][\text{ClO}_4]_2$ and Pigiphos in *cis*-2-pentenitrile gives the *cis*-2-pentenitrile-coordinated Ni complex $[\text{Ni}(\kappa^3\text{-Pigiphos})(\text{NCCH}=\text{CHEt})][\text{ClO}_4]_2$ ($[7][\text{ClO}_4]_2$). The $^{31}\text{P}\{^1\text{H}\}$ NMR spectrum of $[7][\text{ClO}_4]_2$ has broad resonances at 85, 10, and -4 ppm (CyP and two PPh_2 , respectively) and is similar to that of $[3][\text{ClO}_4]_2$. X-ray quality crystals of $[7][\text{ClO}_4]_2$ were obtained by slow diffusion of pentane into a saturated *cis*-2-pentenitrile solution of the complex. The geometries of the two complexes $[3]^{2+}$ and $[7]^{2+}$ with respect to Pigiphos are very similar (see Tables 5 and 6). However, the orientation of the two vinyl nitriles with respect to the Ni(Pigiphos) fragment differ substantially, as illustrated by comparison of the ORTEP diagrams in Figures 2 and 3. Inspection of the trans P2–Ni1–N1 angles (Table 6) shows that $[7]^{2+}$ is less distorted from the ideal square-planar geometry by 10° . Note that in both complexes, this angle primarily corresponds to a vertical displacement of N1 from the plane defined by the three phosphorus atoms. Accordingly, the distance of N1 from this

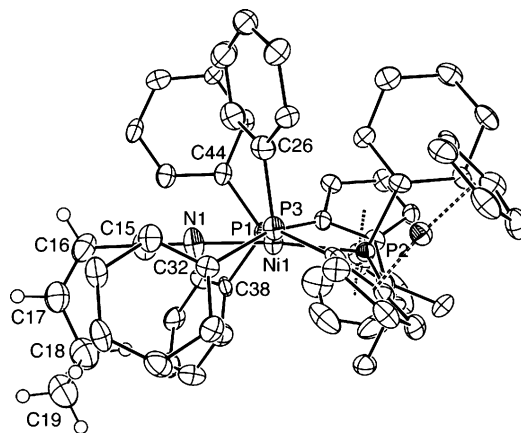


Figure 3. ORTEP diagram of the dication of $[7][\text{ClO}_4]_2 \cdot (\text{NCCH}=\text{CHEt})$, viewed along the P3–Ni1–P1 linear axis (hydrogen atoms of Pigiphos are omitted for clarity; 30% probability ellipsoids). One of the two unsubstituted Cp rings has been found to be disordered and was refined over two positions only one of which is shown, for clarity.

plane in $[7]^{2+}$ is 0.674 \AA , which is 0.475 \AA closer to the phosphorus plane than in $[3]^{2+}$. As a result, the coordinated vinyl nitrile in $[7]^{2+}$ is directed between the pairs of equatorial and axial phenyl groups. For example, the dihedral angles C26–P3–Ni1–N1 and C32–P3–Ni1–N1 ($-82.9(3)$ and $32.1(3)^\circ$, respectively; C26 and C32 are the phenyl *ipso* carbon atoms) indicate that the nitrile nearly bisects the angle of C26–P3–C32. Consequentially, the location of the methacrylonitrile ligand in $[3]^{2+}$ and *cis*-2-pentenitrile ligand in $[7]^{2+}$ differ with respect to the chiral pocket defined by Pigiphos.

Mechanistic Experiments. As mentioned in the Introduction, there are few transition-metal-catalyzed hydrophosphination reactions and even fewer catalytic asymmetric variants of these reactions. Therefore, a mechanistic model for this process is fundamentally interesting and is important for the development of this reaction and other hydrophosphinations. Furthermore, some general observations concerning this reaction, especially with regard to its stereochemistry, are mechanistically intriguing. Importantly, the isolated compound $[3][\text{ClO}_4]_2$ is a catalyst for asymmetric hydrophosphinations and gives similar yields and enantioselectivities as $[1][\text{ClO}_4]_2$ and the in situ-generated catalytic species. As mentioned above, $[3]^{2+}$ is the only Pigiphos-containing species observed in the reaction mixture, and we postulate that it is an intermediate in the catalytic cycle.

The $[3]^{2+}$ -catalyzed reaction of Cy_2PH and methacrylonitrile (as reagent and solvent) was monitored by $^{31}\text{P}\{^1\text{H}\}$ NMR spectroscopy. Although no visible change to the reaction mixture was detected upon addition of 12 equiv of Cy_2PH , $^{31}\text{P}\{^1\text{H}\}$ NMR indicated that 95% conversion occurred within 15 min. A second set of peaks appeared at 34.8 and 34.6 ppm, and a small quantity of Cy_2PH remained even after the mixture was allowed to react for 5 h. At that point, a small resonances at -11.5 ppm appeared. After 5 h, no Pigiphos-containing species could be observed by $^{31}\text{P}\{^1\text{H}\}$ NMR spectroscopy. Additional Cy_2PH did not react, even after 10 days at r.t. When Pigiphos, $[\text{Ni}(\text{H}_2\text{O})_6][\text{ClO}_4]_2$ and $\text{Cy}_2\text{PCH}_2\text{CHMeCN}$ are allowed to react in $\text{THF-}d_8$ overnight, the $^{31}\text{P}\{^1\text{H}\}$ NMR spectrum of the resulting mixture shows peaks corresponding to a nitrile-coordinated $[\text{Ni}(\kappa^3\text{-Pigiphos})(\text{L})]^{2+}$ complex as broad resonances (~ 85 , 14, and 8 ppm) and sharp resonances centered at -11.1 ppm. This observation suggests that small amounts of $[\text{Ni}(\kappa^3\text{-$

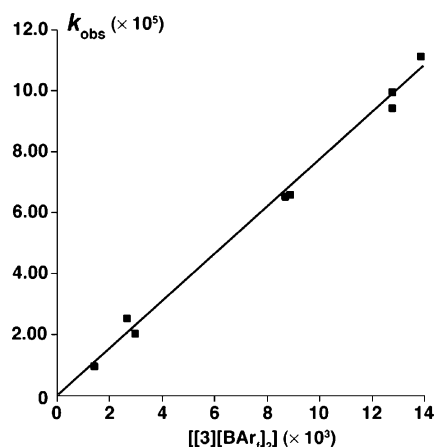


Figure 4. Plot of k_{obs} vs $[3][\text{BARf}_2]$ illustrating first-order dependence on catalyst concentration. Each point represents a second-order rate constant obtained from plots of $\ln\{[\text{methacrylonitrile}]/[t\text{-Bu}_2\text{PH}]\}$ vs time.

Pigiphos($\kappa N\text{-NC}(\text{Me})\text{HCCCH}_2\text{PCy}_2$) $^{2+}$ are formed in the catalytic reaction. Unfortunately, attempts to isolate this compound were unsuccessful.

In contrast, addition of $t\text{-Bu}_2\text{PH}$ (20 equiv) to a methacrylonitrile solution of $[1][\text{ClO}_4]_2$ gives quantitative and rapid conversion (within 10 min) to $t\text{-Bu}_2\text{PCH}_2\text{CHMeCN}$. A $^3\text{1P}\{^1\text{H}\}$ NMR spectrum of the reaction mixture displayed only a singlet corresponding to the product (resonances from Pigiphos and its complexes were not detected). As more $t\text{-Bu}_2\text{PH}$ is added to the reaction mixture, rapid conversion to product occurs (98 equiv relative to $[1]^{2+}$). In these reaction mixtures, intermediate species such as $[3]^{2+}$ and $[\text{Ni}(\text{Pigiphos})(t\text{-Bu}_2\text{PCH}_2\text{CHMeCN})]^{2+}$ are not observed by NMR spectroscopy. In fact, once $t\text{-Bu}_2\text{PH}$ is added to $[3]^{2+}$, the $^3\text{1P}$ NMR signals from Pigiphos-containing species can no longer be detected. However, addition of more $t\text{-Bu}_2\text{PH}$ to these mixture gives the chiral product in high enantioselectivity, that is, the catalytic species is active.

The high activity and selectivity of $t\text{-Bu}_2\text{PH}$ as a substrate in the $[3]^{2+}$ -catalyzed hydrophosphination of methacrylonitrile permitted further mechanistic experiments. Reaction of the deuterium-labeled phosphine $t\text{-Bu}_2\text{PD}$ and methacrylonitrile in the presence of $[3][\text{ClO}_4]_2$ gives the deuterium-labeled product $t\text{-Bu}_2\text{PCH}_2\text{CDMeCN}$ with 90% deuterium incorporation at the methine carbon. Rapid P–D/P–H exchange in the presence of even weak proton sources (including other phosphines and oven-dried glassware) unfortunately prevents possible crossover labeling experiments. The enantiomeric excess of products **2d** and **2d-d₁** synthesized under the same conditions are identical within error.

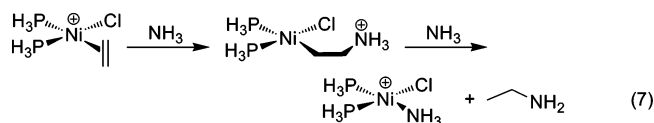
Hydrophosphination reactions, as catalyzed by $[3][\text{BARf}_2]$, were monitored by ^1H NMR spectroscopy (toluene- d_8 , 301 K). The combined use of $[3][\text{BARf}_2]$ and toluene prove critical to obtaining reproducible kinetic data. Pseudo-second-order plots of $\ln\{[t\text{-Bu}_2\text{PH}]/[\text{methacrylonitrile}]\}$ versus time indicate first-order dependence on $[\text{methacrylonitrile}]$ and $[t\text{-Bu}_2\text{PH}]$ (up to 3 half-lives). A plot of k_{obs} versus $[3][\text{BARf}_2]$ (Figure 4) demonstrates first-order dependence on the catalyst, yielding the experimental rate expression: $\text{rate} = k'[3^{2+}][t\text{-Bu}_2\text{PH}][\text{methacrylonitrile}]$ ($k' = 7.73 \times 10^{-3}(4)$ at 28.3 °C). Attempts to investigate the hydrophosphination reaction's kinetics in acetone using $[3][\text{ClO}_4]_2$ as the catalyst were hampered by appreciable product inhibition and difficulties in obtaining

Table 6. ΔE_{rxn} , ΔH_{rxn} , ΔG_{rxn} for the Reaction R_2PH and $\text{H}_2\text{C}=\text{CMeCN}$ to Form $\text{R}_2\text{PCH}_2\text{CHMeCN}$ (in kcal/mol, 298 K)

R	ΔE_{rxn}	ΔH_{rxn}	ΔG_{rxn}
Me	−14.08	−14.44	−2.36
Ph	−12.16	−12.32	0.30
Cy	−11.24	−11.52	1.85
<i>t</i> -Bu	−9.03	−9.40	3.98

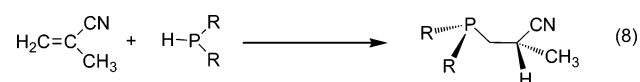
reproducible second-order rate constants. However, it is worth noting that at −20 °C in acetone, the catalyst turnover rate is approximately 10 times higher than in toluene at 28 °C. Additionally, the progress of the reaction of methacrylonitrile and $t\text{-Bu}_2\text{PD}$ was monitored to determine an isotope effect that turned out to be surprisingly high ($k_{\text{H}}/k_{\text{D}} = 4.6(1)$; toluene- d_8 , 28.3 °C) (vide infra).

DFT Calculations on Possible Steps of Hydrophosphination. We hoped to obtain more insight into the mechanism of this hydrophosphination catalysis using DFT calculations. Most relevant to this work is an ab initio study of the Ni(II)-catalyzed addition of ammonia to ethylene.^{15b} In this study, nucleophilic attack of ammonia onto a Ni(II)(η^2 -ethylene) complex gives a pendant ammonioalkyl. The rate-determining step was calculated to require NH_3 -assisted proton transfer from the pendant ammonium ion to the Ni–C bond to give $[(\text{PH}_3)_2(\text{Cl})\text{Ni}-\text{NH}_3]^+$ and $\text{H}_3\text{CCH}_2\text{NH}_2$ (eq 7).



Other hydroamination mechanisms, such as lanthanide-catalyzed hydroaminations/cyclizations and Ti(imido)-catalyzed intermolecular hydroaminations, also have been studied using DFT methods.³⁰

The experimental results described above indicate that the choice of phosphine affects the reaction's efficacy. The secondary phosphines $\text{HP}t\text{-Bu}_2$ and $\text{HP}(\text{1-Ad})_2$ react rapidly and allow high catalyst turnover numbers (>100), while conversions involving HPPH_2 and HPCy_2 give substantially lower catalytic conversions. One possible explanation for this reactivity difference might be that the phosphine substrate markedly impacts the thermodynamics of the addition reaction. Therefore, thermochemistry for the addition of a series of secondary phosphines HPR_2 ($\text{R} = \text{Me}, \text{Ph}, \text{Cy}, t\text{-Bu}$) to methacrylonitrile was calculated (eq 8, values of ΔE_{rxn} , ΔH_{rxn} , and ΔG_{rxn} at 298 K are listed in Table 6).



The hypothetical gas-phase addition of HPMe_2 and $\text{H}_2\text{C}=\text{CMeCN}$ to give the anti-Markovnikov product $\text{Me}_2\text{PCH}_2\text{CHMeCN}$ is slightly exergonic ($\Delta G_{\text{rxn}} = -2.36$ kcal/mol). These calculations indicate that the reactions' thermochemistry does not correlate with our experimental observation that $t\text{-Bu}_2\text{PH}$ is a better substrate than Ph_2PH and Cy_2PH . Although the values for ΔE_{total} and ΔH_{rxn} indicate that the addition is exothermic

(30) (a) Straub, B. F.; Bergman, R. G. *Angew. Chem., Int. Ed.* **2001**, *40*, 4632–4635. (b) Motta, A.; Lanza, G.; Fraga, I. L.; Marks, T. J. *Organometallics* **2004**, *23*, 4097–4104.

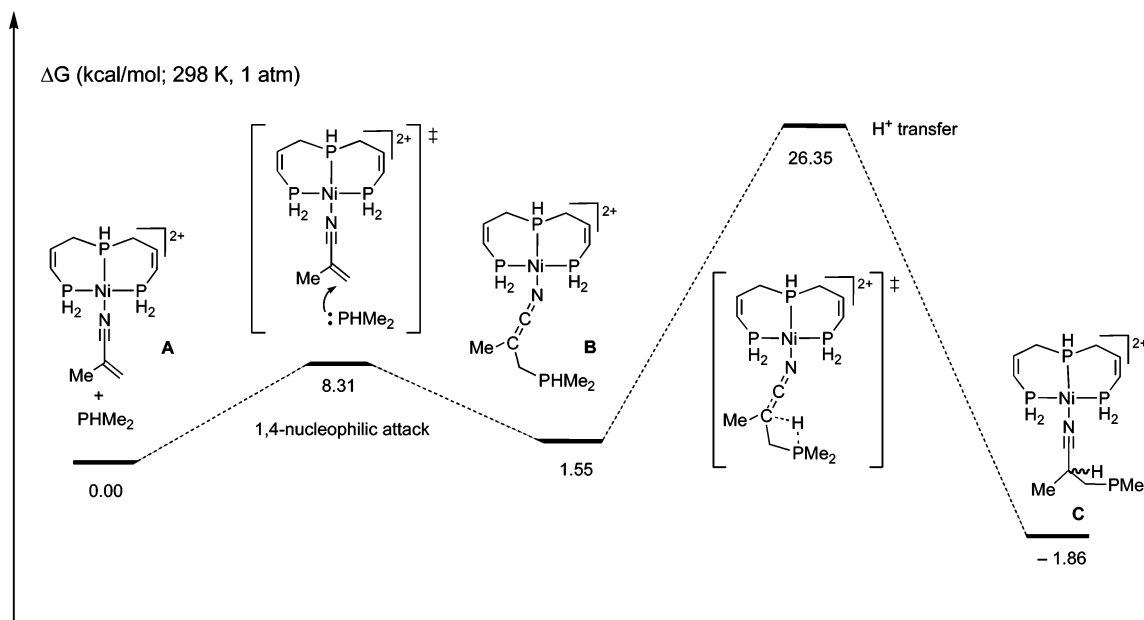


Figure 5. The calculated reaction profile for the Ni(II)-catalyzed addition of HPMe₂ to methacrylonitrile (B3LYP/Ni:lan12dz. P: 6-311+G(d). C, N, H: 6-311G).

by ca. 10–14 kcal/mol, the values for ΔG_{rxn} are calculated to be close to zero or endergonic. Note that olefin hydroamination reactions are frequently estimated to be nearly thermoneutral.³¹

Several modifications to the actual catalytic system were necessary to reduce its complexity to a manageable computational level. The many-atom Pigiphos ligand was approximated as the trisphosphine (H₂PCH=CHCH₂)₂PH. A similar simplification was previously used to model the bidentate ferrocenyl phosphine Josiphos.³² Additionally, the Ni(κ^3 PPP) system was modeled as a dication in the gas phase. Although ligand structure, solvent choice, and counterion effects have been shown experimentally to be important to the rate and selectivity of the hydrophosphination, and these modifications simplify several issues regarding enantioselectivity, these calculations provide valuable insight into aspects of the reaction's mechanism.

The structure [Ni(κ^3 -PH₂CH=CHCH₂)₂PH)(N≡CMeCCH₂)₂]²⁺ (A, see Figure 5 for calculated points on the potential energy surface) was optimized as a model for [3][ClO₄]₂. While the experimentally determined solid-state structure of [3]²⁺ shows a severely distorted square-planar geometry around the Ni center (vide infra), the gas-phase structure is much closer to an idealized geometry (see Tables 7 and 8 for bond lengths and angles of calculated intermediates). It should be noted here that the η^2 -olefin coordination geometry in [Ni(κ^3 -PH₂CH=CHCH₂)₂-PH)(η^2 -H₂CCMeCN)]²⁺ is 45.6 kcal/mol higher in energy than the N-coordinated methacrylonitrile complex and is not expected to be an intermediate on the potential energy surface for hydrophosphination.

Then, the structures [Ni(κ^3 -PH₂CH=CHCH₂)₂PH)N=C=C-(CH₃)CH₂PHMe₂]²⁺ (B) and [Ni(κ^3 -PH₂CH=CHCH₂)₂PH)N≡CC(CH₃)HCH₂PHMe₂]²⁺ (C) were calculated as models for possible intermediates in the hydrophosphination catalytic cycle. Although the coordination geometry of the nitrile ligand is linear

Table 7. Selected Bond Lengths (Å) for the Calculated Gas-Phase Structures [Ni(κ^3 -(H₂PCH=CHCH₂)₂PH)(NCMeC=CH₂)₂]²⁺ (A), [Ni(κ^3 -(H₂PCH=CHCH₂)₂PH)(N=C=CMeCH₂PHMe₂)]²⁺ (B), and [Ni(κ^3 -(H₂PCH=CHCH₂)₂PH)(NCMeHCCH₂PHMe₂)]²⁺ (C)

	A	B	C
Ni1–N1	1.911	1.870	1.903
Ni1–P1	2.277	2.228	2.276
Ni1–P2	2.221	2.256	2.220
Ni1–P3	2.277	2.261	2.276
N1–C15	1.168	1.208	1.166
C15–C16	1.429	1.348	1.464
C16–C18	1.348	1.512	1.551
C16–C17	1.518	1.521	1.562
C17–P4	n.a.	1.849	1.903

Table 8. Selected Bond Angles (deg) for the Calculated Gas-Phase Structure [Ni(κ^3 -(H₂PC=CCH₂)₂PH)(NCMeC=CH₂)₂]²⁺

	A	B	C
N1–Ni1–P2	179.78	171.71	176.66
N1–Ni1–P1	89.02	90.57	90.63
N1–Ni1–P3	89.02	89.94	91.29
P2–Ni1–P1	90.99	91.51	91.26
P2–Ni1–P3	90.97	88.01	87.02
P1–Ni1–P3	177.28	179.49	175.70
Ni1–N1–C15	179.62	153.86	178.01
N1–C15–C16	177.93	172.38	179.58
C16–C17–P4	n.a.	115.31	110.93

in A and C, intermediate B displays a Ni1–N1–C15 angle of 152.9°. The calculated bond lengths of B indicate a stronger Ni1–N1 interaction ($\Delta(\text{Ni1} - \text{N1}) = 0.041$ Å) as the dative nitrile becomes an imino ligand. Additionally, the former nitrile N1–C15 bond length is increased by 0.04 Å and the C15–C16 bond length is decreased by 0.081 Å. Importantly, intermediate B contains a ketenimine structural unit (Ni–N=C=CR¹R²), is therefore chiral, and two energetically equivalent enantiomers exist with the achiral triphosphine used in the model. However, for the actual system containing the chiral ligand Pigiphos two diastereomeric intermediates of differing energy will result upon formation of the P–C bond. The

(31) Brunet, J. J.; Neibecker, D. *Catalytic Heterofunctionalization*; Togni, A., Grützmacher, H., Eds.; VCH: Weinheim, Germany, 2001; pp 91–141.

(32) Magistrato, A.; Woo, T. K.; Togni, A.; Rothlisberger, U. *Organometallics* **2004**, *23*, 3218–3227.

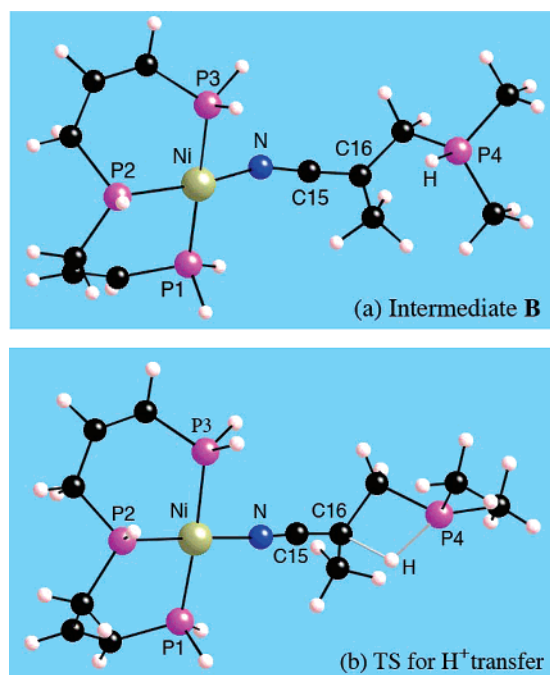


Figure 6. Illustrations of the DFT-calculated structure of (a) the intermediate $((\kappa^3\text{-PH}_2\text{CH=CHCH}_2)_2\text{Ni})\text{-N=C=CMech}_2\text{PHMe}_2$ (**B**) and (b) the calculated transition state for proton transfer (pictures generated using CrystalMaker 6.3.10).

simplified model does not provide any information about how important the relative configurational stability of the ketenimine intermediates will be with respect to the origin of enantioselectivity.

The transition states were also located on the potential energy surface, in particular for the nucleophilic attack of PMe_2H on the 4-position of the methacrylonitrile ligand of **A** and for the proton transfer from the pendant phosphonium group of **B** to the terminal carbon of the ketenimine unit. These two transition states are characterized by exactly one negative mode, as determined by frequency calculations. Interestingly, the higher energy barrier was found for the intramolecular proton-transfer step to give the Ni-coordinated hydrophosphination product **C** (Figure 6). Moreover, the low barriers for phosphine nucleophilic attack and elimination indicate that the initial step is reversible.

Discussion

Metal-catalyzed hydrophosphination is an appealing strategy for stereoselective phosphine synthesis, but as already mentioned, only a few catalytic systems for this transformation have been reported.^{7–10,13} This may be partly related to the near thermoneutrality of the addition reaction, as indicated by our calculations. It is interesting that for transition-metal- and organolanthanide-catalyzed olefin hydrophosphinations, the majority of reports propose a reaction proceeding via the “phosphine-activation” pathway in which formation of a metal–phosphide precedes carbon–phosphorus bond formation.^{7–10} Likely, the alternative olefin-activation pathway (formation of a metal–olefin complex and subsequent nucleophilic attack of the phosphine) is difficult for metal-catalyzed hydrophosphinations because of the competition between olefin and phosphine substrates for coordination to the active site. In this context, Jérôme et al. recently described an interesting alkyne hydro-

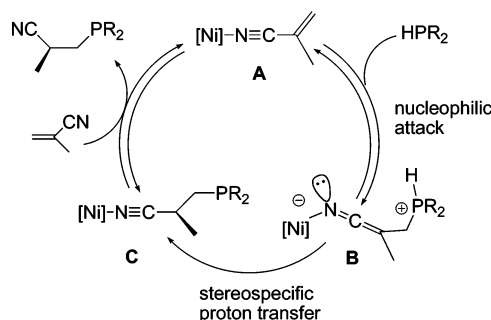


Figure 7. Proposed cycle for $[\text{Ni}(\kappa^3\text{-Pigiphos})(\text{NCMeCCH}_2)]^{2+}$ -catalyzed hydrophosphination of methacrylonitrile.

phosphination catalyzed by $[\text{Cp}^*\text{RuL}_2]^+$ complexes ($\text{Cp}^* = \eta^5\text{-C}_5\text{Me}_5$) in which an electrophilic vinylidene intermediate reacts with a secondary phosphine to give phosphorus–carbon bond formation.³³ Although a metal- $(\eta^2\text{-olefin})$ complex is proposed for a Ni(II)- and Pd(II)-catalyzed hydrophosphination of vinyl ethers, little mechanistic evidence is provided.¹³ Additionally, vinylic phosphines coordinated to a chiral Pd template react to give asymmetric products of hydrophosphination, but this reaction is stoichiometric in Pd.^{12b}

An additional complication inherent to enantioselective hydrophosphination is loss of the chiral ligand from the metal catalyst by ligand substitution, which could be facile and rapid in the presence of a large excess of phosphine under catalytic conditions. Despite several possible complications, a likely mechanism for the $[\text{Ni}(\kappa^3\text{-Pigiphos})(\text{L})]^{2+}$ -catalyzed asymmetric hydrophosphination described here, based on our investigations and supported by DFT calculations, involves a variant of the “olefin-activation” pathway (Figure 7).

Several pieces of experimental evidence support this mechanism. First, experimental observations, which are different from those of the Pt(0)-catalyzed hydrophosphination of acrylonitrile, favor an olefin-activation pathway. The Pt catalysis proceeds readily with sterically undemanding phosphines but does not work well for *t*-Bu₂PH. In contrast, the Ni(II)-catalyzed hydrophosphination is more efficient with bulky secondary phosphines, suggesting that the mechanism does not involve an insertion step. Additionally, a likely intermediate $[\mathbf{3}][\text{ClO}_4]_2$ has been isolated and characterized, in which the methacrylonitrile substrate is coordinated through its nitrogen to the Ni center. This species is an active catalyst for hydrophosphination and gives the same yields, enantioselectivities, and sense of asymmetric induction as the catalyst precursor $[\mathbf{1}][\text{ClO}_4]_2$ or the catalyst generated in situ from $[\text{Ni}(\text{H}_2\text{O})_6][\text{ClO}_4]_2$ and Pigiphos. These observations indeed argue that $[\mathbf{3}]^{2+}$ is an intermediate in the catalytic cycle.

The other two proposed intermediates (**B** and **C**) could not be directly observed, and all attempts to isolate or trap these species were unsuccessful. For example, reaction of $[\mathbf{3}]^{2+}$ with the aprotic nucleophilic phosphides LiPPh_2 , $\text{LiP}(t\text{-Bu})_2$, $\text{KP}(t\text{-Bu})_2$, or LiPMes_2 did not allow isolation or detection of the deprotonated form of intermediate **B**. Additionally, our attempts to prepare intermediate **C**, a Ni(II)Pigiphos complex containing a coordinated $\text{R}_2\text{PCH}_2\text{CHMeCN}$ ligand, were also unsuccessful. However, a mechanism and stereochemical model can be postulated based on our kinetic studies that is supported

(33) Jérôme, F.; Monnier, F.; Lawicka, H.; Dérien, S.; Dixneuf, P. H. *Chem. Commun.* **2003**, 696–697.

by the DFT calculations. The rate law indicates that one methacrylonitrile, one *t*-Bu₂PH, and one Ni center are present in the transition state of the rate-determining step. Moreover, the steps prior to the rate-determining step must be reversible for the reaction to be first order in both [methacrylonitrile] and [*t*-Bu₂PH]. Additionally, for the observed rate law to be consistent with our catalytic cycle, the equilibrium constants for formation of [3]²⁺ (**A**), the ketenimine species **B**, and the Ni product complex **C** must be similar (i.e., saturation of the Ni catalysts as [(κ³-Pigiphos)Ni-methacrylonitrile]²⁺ must not occur). The rate law is consistent with a mechanism commonly described as an ordered ternary-complex mechanism in enzyme kinetics, in which sequential interaction of two substrates and the catalyst gives three equilibrating species prior to an irreversible rate-determining step.³⁴ An alternative mechanism, which involves reversible coordination of a second methacrylonitrile to [3]²⁺ to give a five-coordinate dicationic Ni(II)-(methacrylonitrile)₂ complex, is also consistent with the experimentally determined rate law, particularly if [Ni(κ³-Pigiphos)(methacrylonitrile)]²⁺ is the resting state of the catalytic cycle. However, evidence against coordination of a second methacrylonitrile is found in second-order plots of reactions performed in acetone showing product inhibition. This indicates that the product and methacrylonitrile can compete as ligands for Ni, and therefore the two Ni species [3]²⁺ and [Ni(II)-(product)]²⁺ are likely in equilibrium. Competitive product coordination accounts for the presence of [methacrylonitrile] in the rate equation. Also, this pathway is disfavored by the observation that [Ni(κ³-Pigiphos)Br]⁺ does not catalyze the hydrophosphination and DFT calculations, indicating that coordination of a second methacrylonitrile to the Ni ketenimine intermediate **B** is energetically unfavorable.

The large primary isotope effect proves that the rate-determining step involves cleavage/formation of a bond containing H (or D). Our observations exclude a mechanism involving oxidative addition/insertion/reductive elimination,^{7,8} and we can therefore postulate that proton transfer, as depicted by the calculated transition state shown in Figure 6b, is the rate-determining step. It is possible that the proton-transfer step is assisted by an external base present in the reaction mixture (such as ClO₄[−] or traces of water present in acetone). Unfortunately, attempts to computationally model the possible role of a water molecule, the counteranion ClO₄[−], or acetone solvent have been unsuccessful. However, P⋯H⋯O hydrogen bonds are very weak, and this suggests that a hydrogen-bond-assisted proton transfer is unlikely.^{2a,35} The strongest base that might promote H⁺ transfer present in the reaction mixture is the secondary phosphine. However, the participation of an external phosphine as a proton shuttle in the rate-determining step is not compatible with the observed rate law showing only first-order dependence on phosphine concentration. Also, hydrogen-bonded structures of the type P⋯H⋯P are reportedly disfavored even in environments predisposed to such bridging interactions (e.g., 1-(8-phosphinylnaphthyl)phosphonium triflate).^{35,36}

The isotope effect proves that phosphorus–carbon bond formation is not the rate-determining step, and the rate law

requires that P–C bond formation is reversible. The model compounds and the energy profile of the catalytic cycle calculated by DFT are consistent with this mechanism. In particular, note that the calculated activation barrier for proton transfer is high and the other calculated intermediate species have similar energies.

Interestingly, *t*-Bu₂PH and *t*-Bu₂PD react to give the hydrophosphination product with identical enantiomeric excesses (within error), indicating that the rate of H⁺/D⁺ transfer does not affect the asymmetric induction of the reaction. From this we conclude that the rate-determining step and stereo-determining step do not coincide. The latter step must therefore occur prior to proton transfer. Possible mechanisms for asymmetric induction include stereoselective nucleophilic attack to give unequal amounts of the diastereoisomeric configurationally stable Ni ketenimines **B** (kinetic selectivity). A second possibility involves a rapid equilibrium between these diastereoisomeric intermediates, and our data favors this latter option. First, hydrophosphination of *cis*-2-pentenitrile, in which the enantioselectivity necessarily results from nucleophilic attack, gives the hydrophosphination product in low enantiomeric excess. Second, the kinetic data indicate that P–C bond formation is reversible, and from this we anticipate that the two diastereoisomers are in equilibrium, with the sterically imposing chiral Pigiphos controlling their relative energy. Thus, we postulate that the hydrophosphination's enantioselectivity is related to the formation of two energetically distinct diastereoisomeric intermediates that undergo a rate-determining stereospecific proton transfer. Unfortunately, neither the two diastereoisomers nor model compounds have been isolated and studied to determine if ground state (equilibria between diastereoisomers) or transition state (relative energetic barriers) effects control the stereoselectivity of the hydrophosphinations.

A further important consequence of the sterically hindered tridentate nature of the Pigiphos ligand is that it remains coordinated to the Ni center even in the presence of large excesses of secondary monodentate phosphines (up to 1000 equiv). Additionally, the four phenyls on the peripheral Ph₂P provide substantial steric protection so that coordination of a small elongated ligand such as methacrylonitrile is favored over bulky secondary and tertiary phosphines. This selectivity for vinyl nitrile coordination is, of course, critical to the success of the olefin-activation pathway in this catalytic hydrophosphination.

Conclusion

This report details the successful development of the first highly enantioselective catalytic hydrophosphination reaction. Importantly, we present strong evidence that catalytic hydrophosphination is possible via a metal-mediated olefin-activation pathway. Kinetic data, including a large isotope effect, and DFT calculations provide support for our proposed mechanism. The features of this mechanism include a stereospecific proton-transfer reaction, reversible P–C bond formation, and an unusual Ni ketenimine intermediate.

Although this work primarily focuses on additions of secondary phosphines to methacrylonitrile, we expect that general strategies for new catalytic enantioselective hydrophosphinations might be based on several of the concepts described here. In particular, the strong coordination properties of the tridentate triphosphine Pigiphos is critical to hydrophosphination. Our results also indicate that selective coordination of an olefinic

(34) Laidler, K. J. *Chemical Kinetics*, 3rd Ed.; Harper & Row: New York, 1987; p 405.

(35) Evleth, E. M.; Hamou-Tahra, Z. D.; Kassab, E. *J. Phys. Chem.* **1991**, *95*, 1213–1220.

(36) Reiter, S. A.; Nogai, S. D.; Karaghiosoff, K.; Schmidbaur, H. *J. Am. Chem. Soc.* **2004**, *126*, 15834–15843.

substrate is possible in the presence of a large excess of phosphine. Furthermore, $[1]^{2+}$ is potentially a general catalyst for enantioselective addition reactions of nucleophiles to vinyl nitriles. We have already demonstrated its activity in catalytic additions of amines to such alkenes, and currently we are developing new reactions based on $[\text{Ni}(\kappa^3\text{-Pigiphos})(\text{L})]^{2+}$ -catalyzed additions.

Acknowledgment. Acknowledgment is made to Heinz Rüegger for valuable NMR assistance and to Isabelle Haller for the X-ray structure determinations.

Supporting Information Available: CIF files for the X-ray structures of compounds $[3][\text{ClO}_4]_2 \cdot (\text{NCMeC}=\text{CH}_2)$ and $[7][\text{ClO}_4]_2 \cdot (\text{NCCH}=\text{CHEt})$, spectroscopic data for $[3][\text{BAr}_f]_2$, representative plots showing pseudo-first- and second-order kinetics, and ORTEP diagrams illustrating the absolute configuration of the 2-cyanopropyl-di(*tert*-butyl)phosphine and 2-cyanopropyl-di(1-adamantyl)phosphine products. This material is available free of charge via the Internet at <http://pubs.acs.org>.

JA0555163